

## Review

# Bismuth-213 for targeted radionuclide therapy: from atom to bedside

Stephen Ahenkorah <sup>1,2</sup>, Irwin Cassells <sup>1,2</sup>, Christophe M. Deroose <sup>3,4</sup>, Thomas Cardinaels <sup>1,5</sup>, Andrew R. Burgoyne <sup>1</sup>, Guy Bormans <sup>2</sup>, Maarten Ooms <sup>1,\*</sup> and Frederik Cleeren <sup>2,\*</sup>

<sup>1</sup> Institute for Nuclear Materials Science, Belgian Nuclear Research Center (SCK CEN), 2400 Mol, Belgium; [stephen.ahenkorah@sckcen.be](mailto:stephen.ahenkorah@sckcen.be) (S.A.); [irwin.cassells@sckcen.be](mailto:irwin.cassells@sckcen.be) (I.C.); [thomas.cardinaels@sckcen.be](mailto:thomas.cardinaels@sckcen.be) (T.C.); [andrew.burgoyne@sckcen.be](mailto:andrew.burgoyne@sckcen.be) (A.R.B.), [maarten.ooms@sckcen.be](mailto:maarten.ooms@sckcen.be) (M.O)

<sup>2</sup> Radiopharmaceutical Research, Department of Pharmacy and Pharmacology, KU Leuven, 3000 Leuven, Belgium; [stephen.ahenkorah@kuleuven.be](mailto:stephen.ahenkorah@kuleuven.be) (S.A.); [irwin.cassells@kuleuven.be](mailto:irwin.cassells@kuleuven.be) (I.C.); [guy.bormans@kuleuven.be](mailto:guy.bormans@kuleuven.be) (G.B.); [frederik.cleeren@kuleuven.be](mailto:frederik.cleeren@kuleuven.be) (F.C.)

<sup>3</sup> Nuclear Medicine, University Hospitals Leuven, 3000 Leuven, Belgium; [christophe.deroose@uzleuven.be](mailto:christophe.deroose@uzleuven.be) (C.M.D.)

<sup>4</sup> Nuclear Medicine and Molecular Imaging, Department of Imaging and Pathology, KU Leuven, 3000 Leuven, Belgium; [christophe.deroose@uzleuven.be](mailto:christophe.deroose@uzleuven.be) (C.M.D.)

<sup>5</sup> Department of Chemistry, KU Leuven, 3001 Leuven, Belgium; [thomas.cardinaels@kuleuven.be](mailto:thomas.cardinaels@kuleuven.be) (T.C)

\*Correspondence: [maarten.ooms@sckcen.be](mailto:maarten.ooms@sckcen.be) (M.O) and [frederik.cleeren@kuleuven.be](mailto:frederik.cleeren@kuleuven.be) (F.C)

**Abstract:** Besides external high energy photon or proton beam therapy, targeted radionuclide therapy (TRNT) is an alternative approach to deliver radiation to cancer cells. TRNT is distributed within the body by the vascular system and allows targeted irradiation of a primary tumor and all its metastases, resulting in substantially less collateral damage to normal tissues as compared to external beam radiotherapy (EBRT). It is a systemic cancer therapy, tackling systemic spread of the disease, which is the cause of death in most cancer patients. The  $\alpha$ -emitting radionuclide bismuth-213 ( $^{213}\text{Bi}$ ) has interesting properties and can be considered as a magic bullet for TRNT. The benefits and drawbacks of targeted alpha therapy with  $^{213}\text{Bi}$  are discussed in this review, covering the entire chain from radionuclide production to bedside. First, the radionuclide properties and production of  $^{225}\text{Ac}$  and its daughter  $^{213}\text{Bi}$  are discussed, followed by the fundamental chemical properties of bismuth. Next, an overview of available acyclic and macrocyclic bifunctional chelators for bismuth, and general considerations for designing a  $^{213}\text{Bi}$ -radiopharmaceutical are provided. Finally, we will provide an overview of preclinical and clinical studies involving  $^{213}\text{Bi}$ -radiopharmaceuticals, as well as the future perspectives of this promising cancer treatment option.

**Keywords:** Bismuth-213; Targeted Radionuclide Therapy, Targeted alpha Therapy, radiopharmaceutical; bifunctional chelator; vector molecule

## 1. Introduction

Nuclear medicine plays an important role in the diagnosis, follow-up, and treatment of cancer patients. Radiopharmaceuticals consist conceptually up to three functional elements: 1) a vector (or carrier) molecule with high affinity and selectivity for the target; 2) a radionuclide and 3) a linker or chelator to attach the former to the latter [1–4] (Fig. 1). A fundamental and critical component of a radiometal-based radiopharmaceutical is the chelator, the ligand that binds the radiometal ion in a stable coordination complex so that it can be properly directed to its molecular target *in vivo* [5–7]. The radiopharmaceutical is mostly distributed within the body by the vascular system and allows targeting of a primary tumor and all its metastases. The specific decay characteristics of the radionuclide attached to the vector molecule determine if the radiopharmaceutical can be used for diagnostic (molecular imaging) or therapeutic (TRNT, targeted radionuclide therapy) purposes. The goal of targeted radionuclide therapy is to deliver sufficiently high doses of ionizing radiation to specific disease sites for cure, disease control, or symptomatic (e.g. pain of hormonal secretion) palliation. The biological effect of radionuclide therapy is obtained by three mechanisms: 1) Interaction of ionizing radiation with water in which

chemically active free radicals (reactive oxygen species, ROS) are formed that can react with biomolecules (phospholipids, proteins, RNA, DNA, etc.), thereby irreversibly damaging the cells. 2) Direct interaction of ionizing radiation with DNA in which single-strand (SSB), double-strand (DSB) or cluster breaks can occur. 3) During treatment a phenomenon called the abscopal effect can occur when radiation reduces not only the targeted tumor but also leads to the shrinkage of untreated tumors elsewhere in the body. Though the exact biological mechanisms accountable for the abscopal effect are yet to be identified, the immune system is considered the major player in this significant role [1,8].

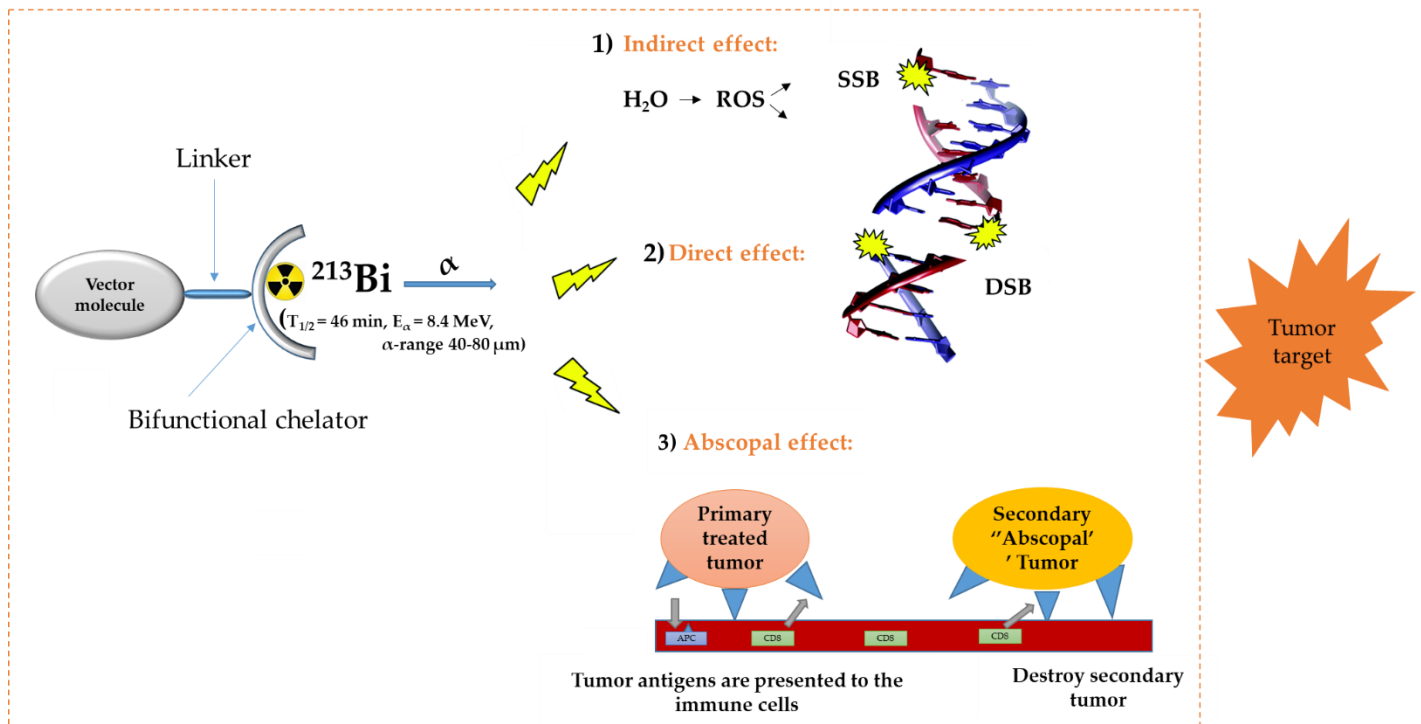


Figure 1: General concept of TRNT. ROS = reactive oxygen species, SSB = single strand break, DSB = double strand break, APC = antigen presenting cells, CD6 = cluster of differentiation 6. The DNA structure was reproduced from Gill M. R and K. A Vallis ,2019, with permission from the Royal Society of Chemistry [9].

Therapeutic radionuclides can be divided into three subgroups:  $\beta^-$ -, Auger- and  $\alpha$ -emitters.  $\alpha$ -decay is a radioactive decay in which a nucleus emits an alpha particle, consisting of two protons and two neutrons. Due to the short penetration depth of  $\alpha$ -particles (50–100  $\mu\text{m}$ , corresponding to a diameter of 2-10 cells), they can selectively destroy tumor cells and cause minimal damage to the surrounding healthy tissue. They are characterized by a high linear-energy transfer (LET, 100  $\text{keV}/\mu\text{m}$ ) and thus a high relative biological effectiveness (RBE). The high LET of  $\alpha$ -particles leads to a high frequency of double-stranded and cluster DNA breaks, and thus irreparable damage, causing the high kill rate of  $\alpha$ -emitting radioisotopes both in normoxic as well as in a hypoxic tumor cell environment, which is known to be more resistant to photon and electron-based irradiation [10]. Therefore, targeted alpha therapy (TAT) can be considered as promising cancer treatment, especially suitable for the treatment of tumors with small diameters and which have a spatially homogeneous expression of the molecule targeted by the vector. Sufficient expression of the target in the malignant tissue must be confirmed before TAT can be initiated. This can be done by first performing a positron emission tomography (PET) or single photon emission computed tomography (SPECT) scan, after injection of the diagnostic sister of the therapeutic radiopharmaceutical. If the diagnostic radiopharmaceutical can truthfully predict the pharmacokinetics of its therapeutic sister, the diagnostic scan also

allows to accurately calculate the dosimetry. This class of radiopharmaceuticals are called theranostic agents [11].

It is also important to mention here that theranostic approach could also involve a solitary radionuclide agent - this theory stipulates the use of a solitary radionuclide, producing both a therapeutic radiation and a low-energy  $\gamma$ -ray for SPECT measurements to deliver dosimetric data. Examples of some of these radionuclides are  $^{47}\text{Sc}$  ( $T_{1/2} = 3.35$  d) and  $^{67}\text{Cu}$  ( $T_{1/2} = 2.58$  d) [12].

The  $\alpha$ -emitting radionuclide  $^{213}\text{Bi}$  ( $T_{1/2} = 45.6$  min,  $E_{\alpha} = 8.4$  MeV,  $\gamma = 440$  keV,  $\alpha$ -particle range = 40-80  $\mu\text{m}$ ) has interesting properties and might be considered as a magic bullet for TRNT [5,9]. However, like every cancer treatment modality,  $^{213}\text{Bi}$ -based TAT has advantages and disadvantages. Indeed,  $^{213}\text{Bi}$  can be considered as powerful precision ammunition, but it needs to be handled with care. In function of the target, the most suited vector molecule needs to be selected and the biological half-life of the vector should be compatible with the 45.6 min physical half-life of  $^{213}\text{Bi}$ , which is substantially shorter than any therapeutic radionuclide in current routine clinical use. Further, an appropriate chelator needs to be carefully chosen in function of the physical properties of  $^{213}\text{Bi}$ .

In this review we will discuss advantages and disadvantages of TAT using  $^{213}\text{Bi}$  covering the entire chain from radionuclide production to bedside. This includes production of the mother isotope  $^{225}\text{Ac}$  and the use of the  $^{225}\text{Ac}/^{213}\text{Bi}$  generator, chemical and physical properties of  $^{213}\text{Bi}$ , an overview of acyclic and macrocyclic chelating agents that are available for  $^{213}\text{Bi}$ , general considerations for designing a  $^{213}\text{Bi}$ -radiopharmaceutical and an in-depth overview of non-clinical and clinical studies that has been performed discussing dosimetry and toxicity issues. Lastly, we will discuss the future perspectives of this intriguing potential cancer treatment.

## 2. Radionuclide properties and production of $^{225}\text{Ac}$ and its daughter $^{213}\text{Bi}$

### 2.1 Decay properties of $^{225}\text{Ac}$ and $^{213}\text{Bi}$

$^{225}\text{Ac}$  is the parent radionuclide of  $^{213}\text{Bi}$  and is a relatively long-lived  $\alpha$ -emitter with a half-life of 9.9 d. It decays via a cascade of six short-lived radionuclide daughters to stable  $^{209}\text{Bi}$  with four net alpha particles emitted per decay (Fig. 2).  $^{213}\text{Bi}$  has a half-life of 45.6 min and shows branching decay ( $\beta^-$  and  $\alpha$  decay), and most of the  $\alpha$ -particles emitted originate from the  $\beta^-$  branch (see Fig. 2). Indeed, it mostly decays via  $\beta^-$  emission to the short-lived  $\alpha$ -emitter  $^{213}\text{Po}$  ( $T_{1/2} = 4.2$   $\mu\text{s}$ ,  $E_{\alpha} = 8.375$  MeV, 97.8%, Fig. 2). The residual 2.2 % of  $^{213}\text{Bi}$  decays leads to  $^{209}\text{Tl}$  ( $E_{\alpha} = 5.549$  MeV, 0.16%,  $E_{\alpha} = 5.869$  MeV, 2.0 %). Finally,  $^{213}\text{Po}$  and  $^{209}\text{Tl}$  decay via  $^{209}\text{Pb}$  ( $T_{1/2} = 3.25$  h,  $\beta^-$ ) to stable  $^{209}\text{Bi}$  [17].

In human tissue, the energy of the  $\alpha$ -particle released by  $^{213}\text{Po}$  (8.375 MeV) has a path length of 85  $\mu\text{m}$ . It is this radionuclide that produces >98% of the  $\alpha$ -particle energy released per disintegration of  $^{213}\text{Bi}$  and could be considered as the radionuclide that provides  $^{213}\text{Bi}$  cytotoxicity. The bulk of the total particle energy released per disintegration of  $^{213}\text{Bi}$  comes from  $\alpha$ -decay, accounting for 92.7 percent, while 7.3 percent comes from  $\beta^-$ -particle emission, which includes the decay of  $^{209}\text{Pb}$  [18]. The decay of  $^{213}\text{Bi}$  is followed by the release of 435 keV (98% abundance) photon which could potentially be used for SPECT gamma cameras with high energy collimators, permitting detailed evaluation of  $^{213}\text{Bi}$  *in vivo* studies [15].

It is noteworthy to mention that high activity  $^{225}\text{Ac}/^{213}\text{Bi}$  generators are required to allow production of clinical amounts of  $^{213}\text{Bi}$ . Optimal clinical injected activities depend on the vector molecules; for prostate-specific membrane antigen (PSMA) targeting radiopharmaceuticals, this has been determined to be 4-8 MBq of  $^{225}\text{Ac}$  [20,21]. In contrast, to have the same number of alpha-particles emitted, a clinical injected activity in the range of 5-10 GBq is needed for  $^{213}\text{Bi}$ -labeled radiopharmaceuticals [22]. This was calculated based on the equations (1 and 2) below and the fact that  $^{225}\text{Ac}$  delivers four  $\alpha$  particles in its total decay scheme while  $^{213}\text{Bi}$  delivers net only one  $\alpha$  particle. Indeed, the much shorter half-life of  $^{213}\text{Bi}$  compared to the half-life of  $^{225}\text{Ac}$  is the key reason for the high activity levels that are needed when using  $^{213}\text{Bi}$  for targeted radionuclide therapy.

$$A = \lambda \cdot N \quad (1)$$

$$\lambda = \ln 2 / T_{1/2} \quad (2)$$

where A = activity (Bq, disintegrations per second) N = number of atoms,  $\lambda$  = decay constant.

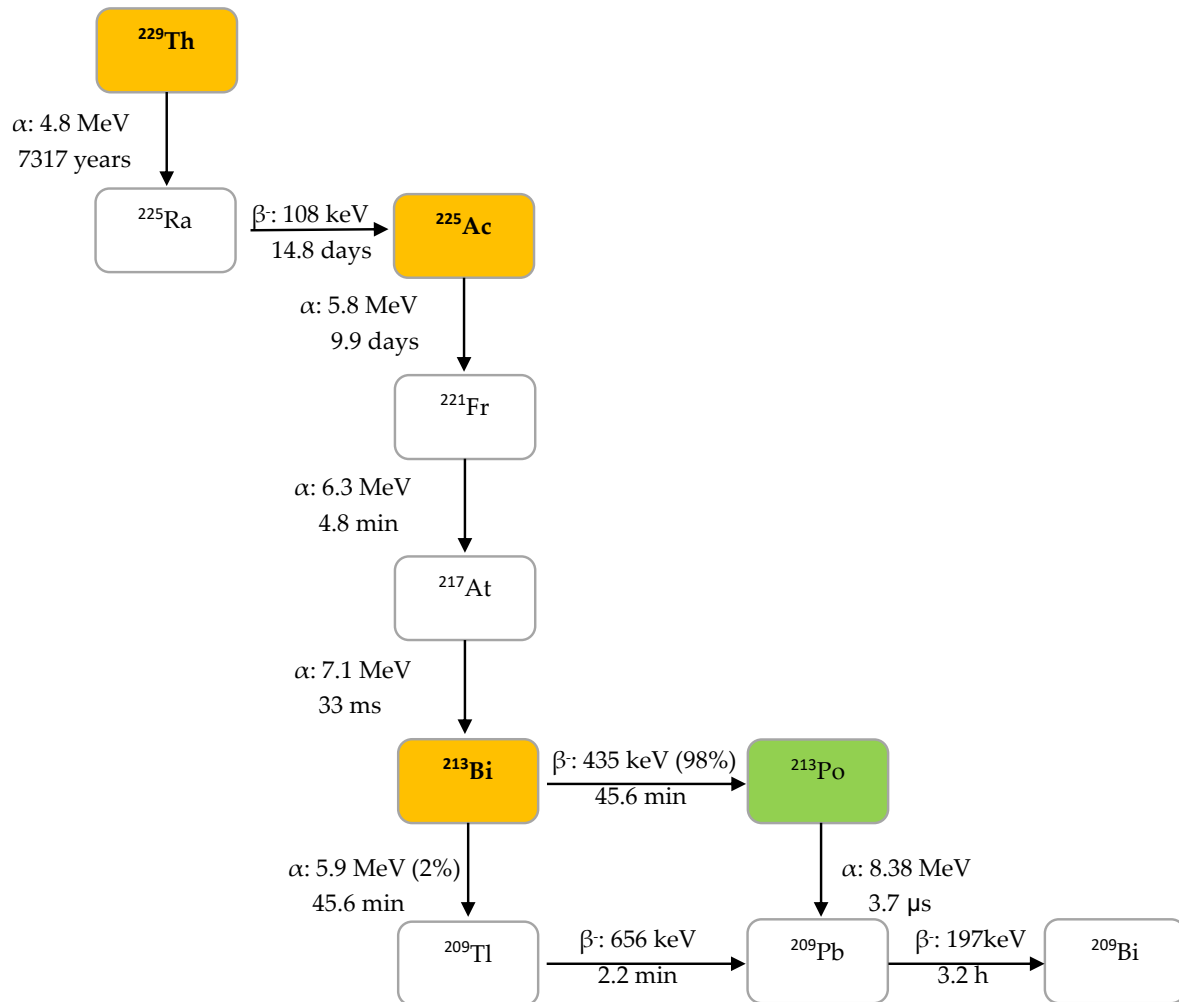


**Figure 2:** Decay chain of thorium-229 to  $^{225}\text{Ac}$  and  $^{213}\text{Bi}$ .

## 2.2 Current strategies for $^{225}\text{Ac}$ production

Several approaches for  $^{225}\text{Ac}$  and  $^{213}\text{Bi}$  production have been recently reviewed and discussed in detail (Fig. 3) [7,17]. The most utilized strategy is the radiochemical extraction of  $^{225}\text{Ac}$  from  $^{229}\text{Th}$  ( $T_{1/2} = 7,317$  y) sources originating from the decay of fissile  $^{233}\text{U}$ . This results in "carrier free"  $^{225}\text{Ac}$  using the generator method, but the available  $^{233}\text{U}$  stocks and thus  $^{229}\text{Th}$  stocks are limited as  $^{233}\text{U}$  management is restricted by the requirements concerning non-proliferation of fissile materials. Most of the  $^{213}\text{Bi}$  and  $^{225}\text{Ac}$  used in clinical tests and research activities worldwide, has so far been produced by this approach [16]. Two examples of  $^{229}\text{Th}$  sources that can produce clinically relevant activities of  $^{225}\text{Ac}$  are (1) the U.S. Department of Energy, Oak Ridge National Laboratory (ORNL) in Oak Ridge, TN, United States of America and (2) Directorate for Nuclear Safety and Security of the JRC of the European Commission in Karlsruhe, Germany. Also at the Belgian Nuclear Research Centre (SCK CEN) in Mol, Belgium, very pure sources of  $^{229}\text{Th}$  were identified, processed, and used for pre-clinical studies [25]. The total annual  $^{225}\text{Ac}$  production volume

is approximately 55-65 GBq [24] and cannot meet the growing demand for  $^{225}\text{Ac}$ , but interestingly, it has been reported that stocks will be increased by extraction of additional  $^{229}\text{Th}$  from US legacy wastes [7].

Cyclotron production is an alternative method for  $^{225}\text{Ac}$  production. Medium-energy proton irradiation of  $^{226}\text{Ra}$  using the reaction  $^{226}\text{Ra}(p, 2n)^{225}\text{Ac}$  is considered to be a viable approach. The advantage of this method is the widespread availability of appropriate cyclotrons worldwide, especially in Europe [26,27] and high amounts of clinical doses of  $^{225}\text{Ac}$  could be produced in a reliable way. It is important to mention that medical cyclotrons used for the production of radioisotopes (15–25 MeV) are considered to be feasible for basic and applied research [28]. The downside with this approach is that  $^{226}\text{Ra}$  is not an easy isotope to work with due to the presence of the highly radiotoxic noble gas  $^{222}\text{Rn}$  in its decay chain. Therefore, it is unlikely that this will ever enter a clinical cyclotron.

Further, high-energy proton irradiation (0.6-2 GeV) of uranium and thorium spallation targets via the reaction  $^{\text{nat}}\text{U}(p, x)^{225}\text{Ac}$  is another approach for the production of  $^{225}\text{Ac}$ . The existence of several suitable high-energy proton facilities makes this an achievable prospect. However, such accelerator-produced  $^{225}\text{Ac}$  contains a low percentage (0.1-0.3%)  $^{227}\text{Ac}$  ( $T_{1/2} = 21.77\text{y}$ ) at the end of bombardment which might be a serious limitation in terms of hospital translation and waste management [29,30]. Nevertheless,  $^{225}\text{Ac}$  obtained through high-energy accelerators could be entirely appropriate for  $^{225}\text{Ac}/^{213}\text{Bi}$  generator production (see 2.3), even with co-production of  $^{227}\text{Ac}$  as all actinium species will be retained on the generator.

Another production path being explored is transmutation of  $^{226}\text{Ra}$  to  $^{229}\text{Th}$  by an intense neutron flux. This will lead to three successive neutron capture reactions:  $^{226}\text{Ra}(n, \gamma)^{227}\text{Ra}$ ,  $^{227}\text{Ac}(n, \gamma)^{228}\text{Ac}$  and  $^{228}\text{Th}(n, \gamma)^{229}\text{Th}$ . However, production of many orders of magnitude of  $^{228}\text{Th}$  ( $T_{1/2} = 1.9\text{y}$ ) intermediate and handling of the radium target remains a challenge [22].

$^{226}\text{Ra}(\gamma, n)^{225}\text{Ra}$  is another reaction path for  $^{225}\text{Ac}$  production which has been determined experimentally [33,34]. This strategy explored irradiation of an old radium needles on electron linear accelerators (linacs) located in most recent cancer centres.

Finally, transmutation of  $^{226}\text{Ra}$  to  $^{225}\text{Ra}$  by fast neutrons via the reaction  $^{226}\text{Ra}(n, 2n)^{225}\text{Ra}$  is also under consideration. It is noteworthy to point out that the limitation for all the strategies discussed is the handling of the radium targets. However, earlier results with these methods have been promising [26].

To conclude, all clinical studies with  $^{225}\text{Ac}/^{213}\text{Bi}$  radiopharmaceuticals were performed to date with  $^{225}\text{Ac}$  originating from  $^{229}\text{Th}$  stocks, but other accelerator-based production routes were heavily investigated the last decade. This progress will hopefully assure reliable production and delivery of  $^{225}\text{Ac}$  to radiopharmacy institutes in the near future allowing more preclinical research and multicentre clinical trials with both  $^{225}\text{Ac}$  and  $^{213}\text{Bi}$ -radiopharmaceuticals.

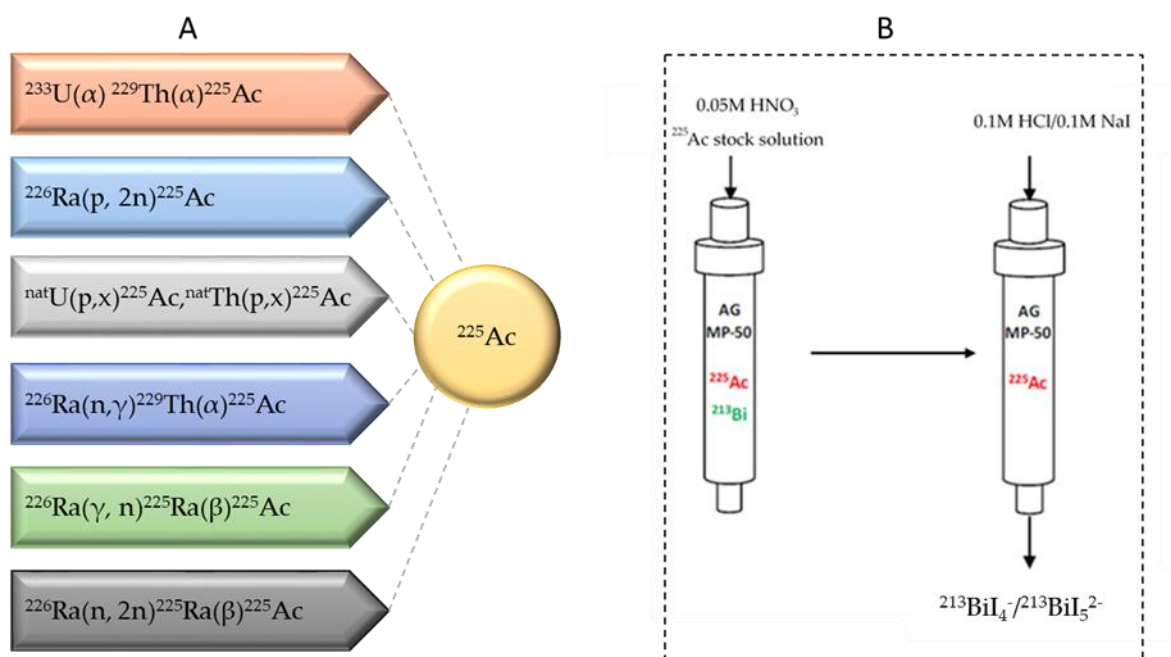


Figure 3: (A) Production routes for  $^{225}\text{Ac}$  and (B) the  $^{225}\text{Ac}/^{213}\text{Bi}$  generator

### 2.3 $^{225}\text{Ac}/^{213}\text{Bi}$ Radionuclide Generators

$^{225}\text{Ac}$  can be loaded on  $^{225}\text{Ac}/^{213}\text{Bi}$  generators to deliver  $^{213}\text{Bi}$  on site, but it can also be used directly as a therapeutic radionuclide.  $^{225}\text{Ac}/^{213}\text{Bi}$  generators are well explored and discussed [37–39]. The most established strategy is based on the direct generator method in which the parent  $^{225}\text{Ac}$  in acidic solution (e.g. 0.05M  $\text{HNO}_3$ ) is strongly retained by the sorbent (e.g. AG MP-50 cation exchange resin) and  $^{213}\text{Bi}$  is eluted. Elution is performed generally with a mixture of 0.1M  $\text{HCl}/0.1\text{M NaI}$  to obtain  $^{213}\text{Bi}$  in the form of  $^{213}\text{BiI}_4$  and  $^{213}\text{BiI}_5^{2-}$  that can be directly used for radiochemistry purposes. (Fig. 3) [7]. These generators have clinically promising qualities due to the relatively long parent half-life which allows shipment of the generator towards radiopharmacy facilities at long distance. Also, the transient equilibrium of the  $^{225}\text{Ac}$ – $^{213}\text{Bi}$  permits elution at approximately every 3 h [40]. These generators can provide weeks of reliable in-house generation of  $^{213}\text{Bi}$  for radiolabeling purposes [41]. High activity (up to 4 GBq  $^{225}\text{Ac}$ ) generator systems, developed at JRC Karlsruhe, have been reported with yields of  $^{213}\text{Bi}$  elution exceeding 80% and low breakthrough of  $^{225}\text{Ac}$  of less than 0.2 ppm [40].

## 3. Fundamental chemistry of Bi

Bi is an element that in comparison to the lighter main group metals has received only limited attention in the past. However, Bi compounds are used in a wide spectrum of applications ranging from non-toxic pigments and catalysts to biocompatible additives in dental materials and remedies in human and veterinary medicine [42,43]. To select a good chelator for  $^{213}\text{Bi}$  to be used in radiopharmaceutical applications, it is important to have an in-depth knowledge about the chemical properties of Bi.

The Bi atom has 83 electrons distributed among different energy levels. Electrons occupying the highest and outermost energy levels are responsible for its chemical reactivity [42]. Bi has a  $[\text{Xe}] 4f^{14}5d^{10}6s^26p^3$  electron configuration and tends to form trivalent bismuth ( $\text{Bi}^{3+}$ ) with  $6s^2$  valence configuration. For this tendency of the  $6s^2$  electron pair to remain formally unoxidized in Bi compounds (i.e core-like nature of the  $6s$  electrons), the term “inert pair effect” [44], or ‘nonhybridization effect’ has often been used [45]. Bi has two major oxidation states (III and V) with Bi(III) being the most common and stable oxidation state. However, rare occurrences of Bi(II) and Bi(IV) has been reported [46].

The aqueous Bi chemistry is predominantly dominated by Bi(III) and unlike the d-block metals, Bi forms complicated, clustered structures across the pH scale [47,48]. At

low pH, Bi(III) ( $pK_{a1} = 1.5$ ) readily undergoes hydrolysis to form Bi(III) hydroxide [49]. For e.g in dilute solutions ( $[Bi] < 1 \times 10^{-5}$  molality), mononuclear complexes predominate considerably over a wide range of pH values [50]. These mononuclear complexes of Bi largely follow a stepwise addition of  $OH^-$  such that  $Bi(OH)_x^{(3-x)}$  (where  $x < 4$ ) complexes are formed sequentially with increasing pH. Increasing the acid concentration prohibit the formation of the Bi crystal structures, which is expected as polyaqua Bi(III) is the major form at low pH [47].

Bi(III) is a borderline metal ion, according to Pearson's hard-soft acid-base (HSAB) theory [51]. Nevertheless, with considerable affinity for nitrogen and oxygen donor atoms [52–54], some researchers have reported Bi(III) as a strong Lewis acid [47]. This property makes complexation with amine donor groups possible even at low pH [55]. The complexation kinetics with N- and O- donor atoms is often fast, with equilibrium achieved in a few minutes [55]. Some amino ligand binding constants have predictive nature, which can be expressed as  $\log K_1(\text{polyamine}) = 1.152 \log \beta_n(NH_3) + (n-1) \times 1.744$ , where  $\beta_n$  refers to the stability of the complex containing primary amine analogues and  $n$  is the number of primary amine analogues of the polyamine [55]. As observed with aqua ligands, small O-donor ligands bridge multiple Bi atoms to form cluster species [56].

In Bi coordination chemistry, Bi(III) complexes exhibit a number of coordination numbers, with values between 3 – 10 [49]. Low coordination numbers can be well-predicted using valence shell electron pair repulsion theory (VSEPR, see **Table 1**) [49]. Nonetheless, higher coordination numbers ( $>6$ ) require more complex levels of theory to account for structural influence on geometry (e.g. vibrational coupling, etc.).

Table 1. Summary of geometries for each coordination number [49].

Coordination number	Geometry	Example
3	Pyramidal	$Bi(SAr)_3$
4	Trigonal bipyramidal	$[Bi\{OP(NMe_2)_3\}_2][Fe(CO)_2(\eta^5-Cp)_5F_2][PF_6]$
5	Square-based pyramidal	$Na_2[Bi(SC_6F_5)_5](THF)_4$
5	Trigonal antiprism	$\{Bi(NO_3)bis[1-azepanyl-4-(2-thienyl)-2,3-diazapenta-1,3 diene-1-thiolato-N^3,S]\}$
6	Octahedral	$[Bi_6O_4(OH_4)]$
7	Trigonal Dodecahedron	$\{Bi(NO_3)bis[1-azepanyl-4-(2-pyridyl)-2,3-diazapenta-1,3 diene-1-thiolato-N',N^3,S]\}$
8	Bicapped trigonal prism	$[Bi(nta)(H_2O)_2]$
9	Tricapped trigonal prism	$[Bi(H_2O)_9](CF_3SO_3)$
9	Monocapped square antiprism	$(guanidinium)_2[Bi(dtpa)] \cdot 4H_2O$

4. Bifunctional chelating ligands for <sup>213</sup>Bi

In radiometal-based radiopharmaceuticals a bifunctional (BF) chelator is required, which is a chelator with a reactive functional group. This BF ensures a covalent bond with the vector molecule and forms a stable complex with the radiometal. Because of the high cost of the  $\alpha$ -emitting radionuclides, short physical half-life in the case of <sup>213</sup>Bi and radio-protection reasons, quantitative yields using fast and mild radiolabeling conditions (e.g. room temperature, 5 min) are desired to facilitate efficient good manufacturing production (GMP)-compliant on-site production of <sup>213</sup>Bi radiopharmaceuticals. Further, if the vector molecule is a heat-sensitive biomolecule or peptide, mild aqueous labelling conditions

should be applied to avoid degradation of the vector molecule. Importantly, the radio-metal-chelator complex should have a high thermodynamic stability and kinetic inertness to avoid *in vivo* dissociation that typically occurs via transchelation to serum proteins and enzymes. Several papers have reported that naked  $^{213}\text{Bi}$  and  $^{213}\text{Bi}$  dissociated from its chelating ligands tend to accumulate in the kidney [5,57,58]. In this chapter, we will give an overview of most important bifunctional chelators currently used for  $\text{Bi}^{3+}$ .

#### 4.1 DTPA and DTPA-derivatives

The discovery of acyclic chelators with rapid radiometal ion coordination kinetics, high *in vivo* stability, and kinetic inertness has become a requirement for TRNT due to the emergence of antibody vectors.

As one of the oldest chelators used in radiopharmaceuticals, BF diethylenetriamine-*N,N,N',N',N'*-pentaacetic acid (DTPA) (Fig. 5B) can rapidly radiolabel different radiometal ions, even at room temperature [3]. However, *in vivo* stability remains the major limitation and is generally not as stable as the radiometal complex with DOTA (1,4,7,10-tetraazacyclododecane-1,4,7,10-tetraacetic acid, Fig. 5C). BF-DTPA has been used successfully with the FDA approved SPECT agent  $^{111}\text{In}$ -DTPA-octreotide (OctreoScan<sup>TM</sup>, a somatostatin receptor targeting peptide-conjugate used for imaging neuroendocrine tumors [3,59]. Also, it has been successfully radiolabeled with different radiometals such as  $^{213}\text{Bi}$ ,  $^{111}\text{In}$ ,  $^{177}\text{Lu}$ ,  $^{64}\text{Cu}$ , and  $^{86/90}\text{Y}$ , but has been made superfluous by the introduction of more stable DTPA-derivatives like 1B4M-DTPA and BF-CHX-A''-DTPA (Fig. 5A) [2,3]. BF-1B4M-DTPA (Fig. 5B), a DTPA derivative that contains a single methyl group on one of its ethylene backbones has been successfully used for the FDA-approved  $^{90}\text{Y}$  therapeutic immunoconjugate ibritumomab tiuxetan (BF-1B4M-DTPA, Zevalin<sup>®</sup>) [60]. The presence of the cyclohexyl moiety of CHX-A''-DTPA provides the chelator with additional rigidity and imposes a significant degree of preorganization on the metal ion binding site, augmenting kinetic inertness, but impeding radiolabeling kinetics as compared to DTPA [3].

While kidney uptake is problematic with DTPA, caused by *in vivo* dissociation of  $^{213}\text{Bi}$  from the chelator, [61] a slight improvement is recorded with  $^{213}\text{Bi}$ (1B4M-DTPA). Owing to its equivalent stability with DTPA, current  $^{213}\text{Bi}$  TAT research mostly uses CHX-A''-DTPA ( $\log K_{ML} = 34.9\text{--}35.6$ ) [61,62], which has significantly improved inertness when complexed with trivalent Bi. A clear backbone rigidity effect on  $^{206}\text{Bi}$  release was observed after a study comparing renal uptake of B72.3-mAb radiolabeled with  $^{206}\text{Bi}$  using DTPA, CHX-A''-DTPA and 1B4M-DTPA as chelating ligands. Kidney uptake amounted to 27.2 %ID/g for DTPA, 7.8 %ID/g for CHX-A''-DTPA and 13.2 %ID/g for BF-1B4M-DTPA respectively [63]. CHX-A''-DTPA displayed considerably superior stability over DTPA; however, its stability could still not match with that of DOTA. For example in mice injected with  $^{88}\text{Y}$ -(DOTA)-B3, cortical bone up take at 168 h was five times less than that observed for  $^{88}\text{Y}$ -(CHX-A''-DTPA)-B3 and the authors concluded that bone uptake of radioyttrium can be significantly reduced by using the DOTA instead CHX-A''-DTPA [64]. Complex geometry and thermodynamic parameters of  $^{213}\text{Bi}$  with different chelators are summarised in table 2.

#### 4.2 DOTA and DOTA-derivatives

The current "gold standard" BF chelator for  $^{213}\text{Bi}$  is the amino carboxylate macrocycle DOTA and  $^{213}\text{Bi}$ -DOTA bioconjugates have been reported to be stable *in vitro* and *in vivo* for at least two hours [65,66].  $\text{Bi}^{3+}$  adopts a square antiprism geometry with DOTA in the [Bi-DOTA]-complex (see Fig. 4) [67]. Despite the high thermodynamic stability of the  $^{213}\text{Bi}$ -DOTA complex ( $\log K_{ML} = 30.3$ ), DOTA has several drawbacks as a  $^{213}\text{Bi}$  chelator. DOTA's typical radiolabeling conditions require heating at high temperatures (e.g. 30-60 min at 95 °C) at pH 4-9, depending on the type of buffer used. Additionally, it has been demonstrated that a high concentration of DOTA (10  $\mu\text{M}$ ) is required to achieve quantitative

yields for  $^{213}\text{Bi}$ -labeling. In contrast, for CHX-A''-DTPA, a concentration of 1  $\mu\text{M}$  is in general sufficient to achieve quantitative yields [68]. The relative short half-life of  $^{213}\text{Bi}$  requires short radiolabeling times, which is not the case for DOTA and results in significant loss of radioactivity due to decay. Additionally, the high temperatures are unsuitable for heat-sensitive proteins of interest for TRNT as this may cause the proteins to denature.

BF-PEPA (Fig. 5E), a chelator which is an expanded version of DOTA has also been studied with  $^{205/206}\text{Bi}$ . This chelator was developed to improve the formation kinetics of Bi-DOTA radiocomplexes. Unfortunately this chelator was discovered not to be ideal for Bi and this was as result of the lower tumor uptake and increased kidney uptake of the  $^{205,206}\text{Bi}$ -B3-PEPA [58].

Me-DO2PA (Fig. 5D), a [12]aneN4 bearing two picolinic acid arms and two methyl-capped amines has also been reported to be stable *in vivo* when radiolabeled with  $^{213}\text{Bi}$  [69,70]. Even though DOTA-derivatives have shown promising results as  $^{213}\text{Bi}$  chelators, other options have been explored.

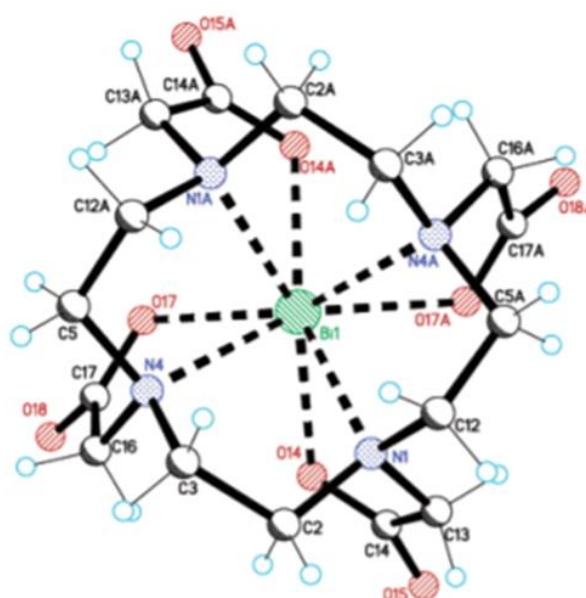


**Figure 4**, Crystal structure of NaBiDOTA·H<sub>2</sub>O. Reprinted (adapted) from E. Brücher *et. al.*, 2003 with permission from (ACS). Copyright (2003) American Chemical Society [67].

#### 4.3 NETA and DEPA-derivatives

NETA (4-[2-(bis-carboxymethyl-amino)-ethyl]-7-carboxymethyl-[1,4,7]triazonan-1-yl)-acetic acid, Fig. 5G)) and DEPA (7-[2-(bis-carboxymethyl-amino)-ethyl]-4,10-bis-carboxymethyl-1,4,7,10-tetraazacyclododec-1-yl)-acetic acid, Fig. 5H) are promising chelators for radionuclide therapy of  $\alpha$ - and  $\beta$ -emitters including  $^{90}\text{Y}$ ,  $^{177}\text{Lu}$  ( $T_{1/2} = 6.7$  d),  $^{206}\text{Bi}$ ,  $^{207}\text{Bi}$ ,  $^{213}\text{Bi}$  and  $^{212}\text{Pb}$ . NETA possesses both a parent macrocyclic NOTA (1,4,7-triazacyclononane-*N,N',N''*-triacetic acid) backbone and a flexible acyclic tridentate pendant arm (DTPA). DEPA on the other hand is made up a donor system incorporating both macrocyclic DOTA and acyclic tridentate pendant arm (DTPA). The idea of designing NETA/DEPA was to integrate the advantage of both the macrocyclic and acyclic frameworks, i.e., rapid complexation (favourable formation kinetics) at ambient temperatures with radionuclides, and high thermodynamic stability [71,72].

$^{205/206}\text{Bi}$ -NETA analogue displayed a lower degree of degradation compared to CHX-A''-DTPA after *in vitro* challenge experiments [66]. Biodistribution experiments of unconjugated [ $^{205/206}\text{Bi}(\text{C-NE}3\text{TA})$ ]- in non-tumor-bearing mice showed a high level of kidney uptake ( $24.63 \pm 2.79$  %ID/g) after one hour. However, a biodistribution studies of a seven-coordinate analogue [ $^{205/206}\text{Bi}(\text{C-NE}3\text{TA})$ ] resulted in reduced kidney uptake ( $4.69 \pm 0.55$  %ID/g) even though a seemingly non-coordinatively saturated  $\text{Bi}^{3+}$  metal centre [71,74]. A version of NETA with a prolonged linker between the coordinating functional

groups and pendant isothiocyanate group (*p*-SCN-Bn) in the subsequent experiments stipulates that the instability could originate from coupling group interference. 3p-C-NETA-trastuzumab displayed rapid labeling of  $^{205/206}\text{Bi}$  to DOTA-trastuzumab, and in vivo experiment on mice bearing subcutaneous tumors (LS-174T, which expresses HER-2, the target of trastuzumab) demonstrated significant tumor accumulation without increasing kidney uptake (after 24 h) [75]. This study showed that 3p-C-NETA could be radiolabeled at room temperature to produce quantitative yield with high stability in vitro and in vivo, which is not possible with DOTA.

The  $^{205/206}\text{Bi}$ -DEPA complex has also been studied to show similarly promising results with DTPA as benchmark [76,77]. After 72 h time point  $^{205/206}\text{Bi}$ -C-DEPA-trastuzumab remained 100% intact in human serum. However, in the case of  $^{205/206}\text{Bi}$ -DTPA-trastuzumab only 77% was intact after 72 h [76].  $^{205/206}\text{Bi}$ -3p-C-DEPA-trastuzumab also showed significant tumor uptake in tumor-bearing (LS-174T) mice. As suggested by Price and Orvig, an in depth assessment of NETA versus DEPA (Fig. 5E) for Bi-based bioconjugates might be useful to identify the “gold standard” of Bi chelators [3]. Finally, a promising bifunctional picolinic acid-based scaffold chelator, H4neunpa (Fig. 5F) has also been studied. The only concern is that the stability with  $\text{Bi}^{3+}$  ( $\log K_{\text{ML}} = 28.8$ ) was discovered to be lower than that of DOTA and DTPA, however, the pM value is the similar to that of DOTA (pM = 27), providing favourable evidence for in vivo use.

Table 2. Overview of  $\text{Bi}^{3+}$  Chelators, Complex Geometry and Thermodynamic Parameters [2].

Metal ion	Ligand	Coordinating nuclei	Geometry	$\log K_{\text{ML}}^b$	pM <sup>c</sup>
$\text{Bi}^{3+}$	DOTA	$\text{N}_4\text{O}_4$	Square antiprism	30.3	27.0
$\text{Bi}^{3+}$	Me-DO2PA	$\text{N}_6\text{O}_2$	Square antiprism	34.2	28.6
$\text{Bi}^{3+}$	DTPA	$\text{N}_3\text{O}_5$	Square antiprism	33.9-35.2	-
$\text{Bi}^{3+}$	CHX-DTPA	$\text{N}_3\text{O}_5$	Square antiprism	34.9-35.6	-
$\text{Bi}^{3+}$	NETA	$\text{N}_4\text{O}_4$	Square antiprism	-	-
$\text{Bi}^{3+}$	DEPA	$\text{N}_4\text{O}_5/\text{N}_5\text{O}_4^a$	Distorted dodecahedron	-	-
$\text{Bi}^{3+}$	H4neunpa	$\text{N}_5\text{O}_4$	Distorted dodecahedron	28.8	-

<sup>a</sup> under investigation, <sup>b</sup>  $K_{\text{ML}}$  represents the formation constant of the metal complex, <sup>c</sup>pM value is the negative log of the concentration of free metal ion uncomplexed by a given chelator under specific conditions.

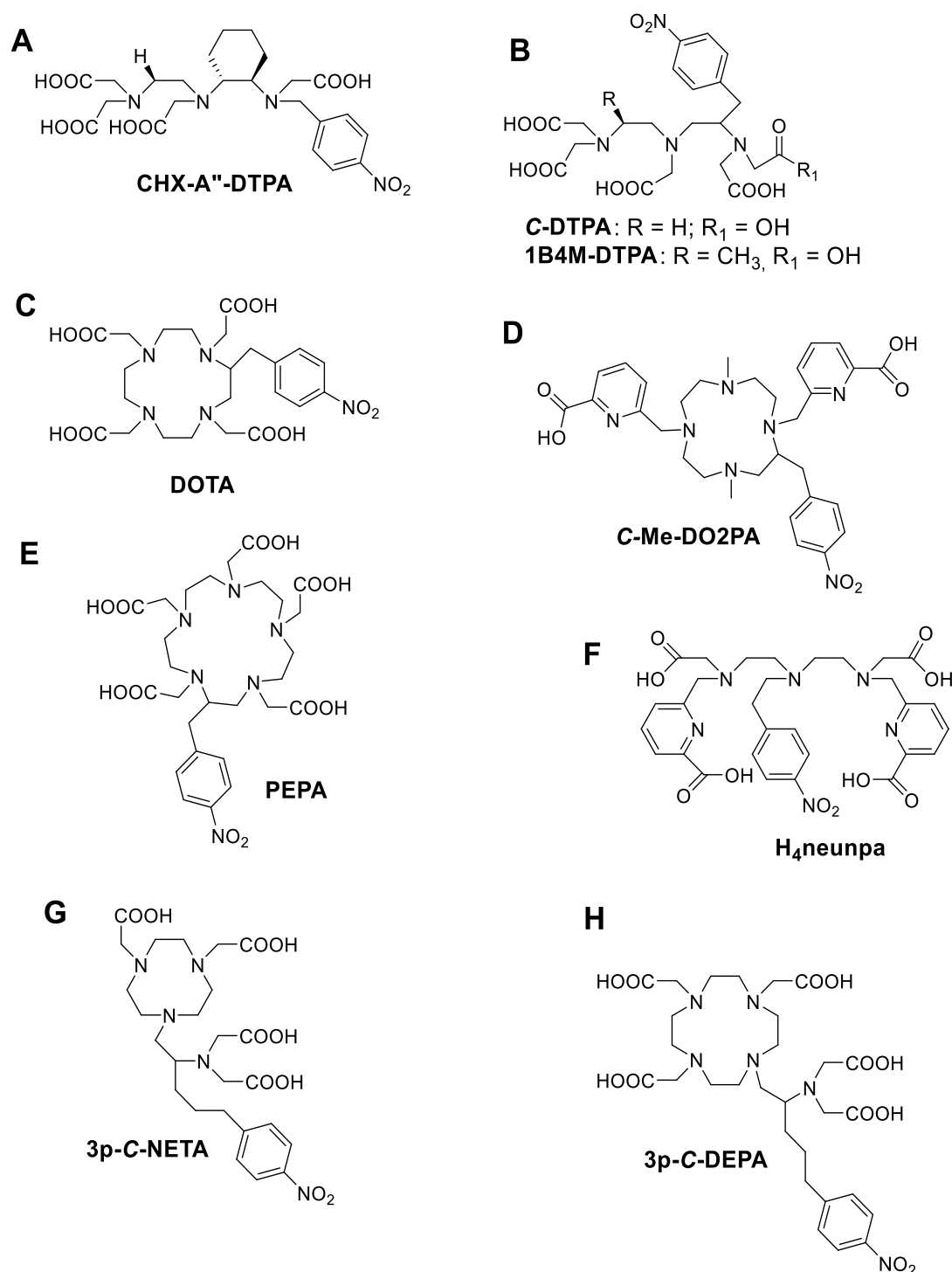


**Figure 5,** Some structures of bifunctional chelators currently used for  $^{213}\text{Bi}$

### 5. General considerations for designing a $^{213}\text{Bi}$ -radiopharmaceutical

In order to realize the potential and favourable properties of  $^{213}\text{Bi}$ , specifically targeted carriers need to be developed [1,3,4]. Indeed, the vector molecule is an essential part of the therapeutic radiopharmaceutical as it is responsible for the selective interaction with the target leading to a high concentration of the radionuclide in the target tissue. The target of interest should have sufficiently high differential expression in the target tissue versus the background tissue combined with sufficiently high absolute expression ( $B_{\text{max}}$ ). Several of these traceable targets are currently being used for TAT with  $^{213}\text{Bi}$ -labeled probes such as human epidermal growth factor receptor 2 (HER2) [78], cluster of differentiation

20 (CD20) [79], CD33 [80,81], CD45 [82], substance P [83–85], somatostatin receptors [16,66], prostate-specific membrane antigen (PSMA) [86], and epidermal growth factor receptor (EGFR) [13].

The retention in the target tissue can be due to a reversible interaction such as affinity-based receptor or transporter binding, governed by equilibrium association and dissociation. After binding to the target, the tracer may however be internalized and retained in the cell. This internalization can be beneficial since it leads to pseudo-irreversible kinetics which maximize selective irradiation of the tumor tissue.

In general, radiopharmaceuticals are administered intravenously and will quickly distribute over the body and due to physical or chemical interaction they will concentrate in the target tissue or cells. The concentration of the radiopharmaceutical in surrounding tissue, which lacks the interaction mechanism, will be in equilibrium with the plasma concentration that will decrease due to clearance of the radiopharmaceutical from plasma by excretory organs such as liver and kidneys. For oncological applications and especially in the case of TAT using  $^{213}\text{Bi}$ , renal clearance and urinary excretion is preferred over hepatobiliary clearance, since the latter results in a slow transfer through the gastro-intestinal tract which results in high activity levels in the abdomen.

The vector molecule can consist of a small organic molecule, a peptide, a protein including antibodies and antibody fragments (Fig. 6) [4]. It is important that the vector molecule has a high affinity and selectivity for the target and maintains this affinity and selectivity after conjugation with the radionuclide. As  $^{213}\text{Bi}$  is a radiometal, derivatization of small organic molecules with a bulky chelator usually significantly alter its binding properties. Therefore, mostly peptides and antibody fragments are used as vector molecule in  $^{213}\text{Bi}$ -labeled radiopharmaceuticals. Their large size and the presence of non-binding pockets usually make them less sensitive to changes in target affinity when being derivatized with bulky bifunctional ligands.

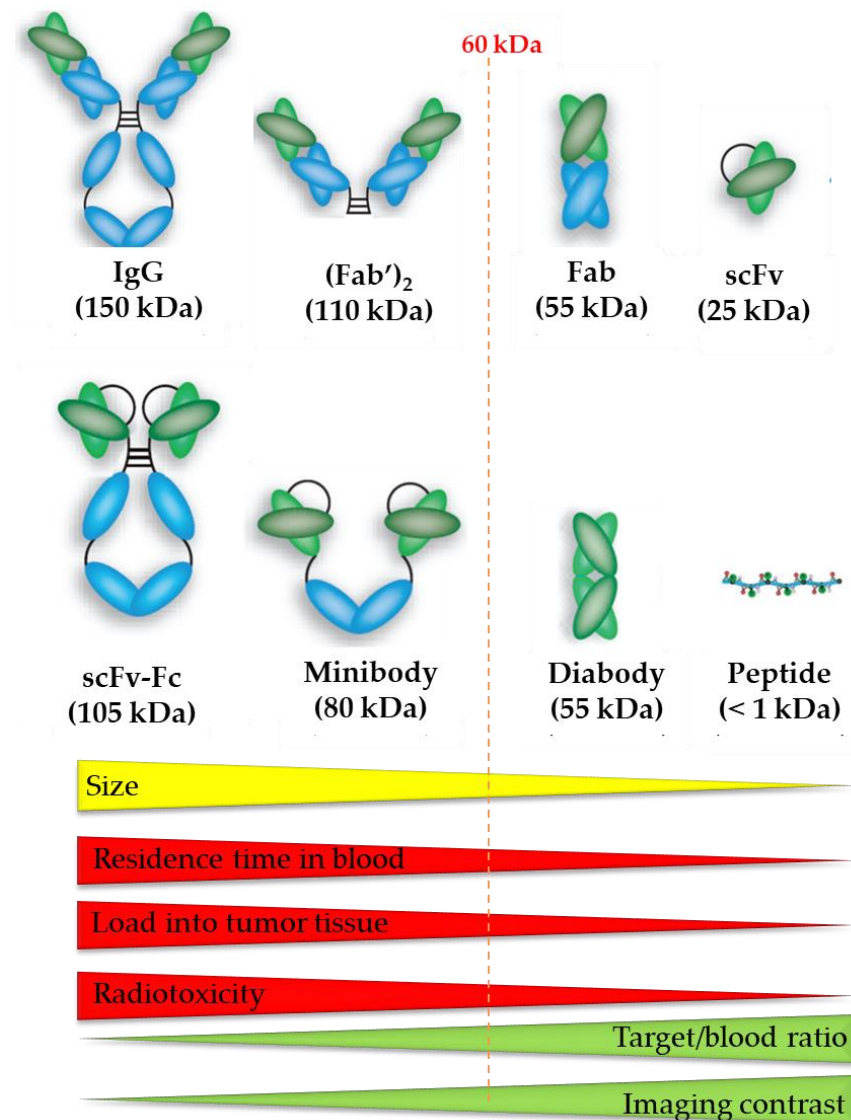


Figure 6. The size of the vector molecule determines the residence time of blood, tumor accumulation, radiotoxicity, target-to-blood ratio, and imaging contrast of the radiopharmaceutical. Image was adapted and modified with permission from Cai W *et al.*, 2008 [87].

An important factor when assessing therapeutic potential of vectors is the kinetic profile of the carrier. In general, the vector molecules with longer circulation time in blood have the highest tumor accumulation, which is beneficial for the efficacy of TAT treatment. On the other hand, longer residence time in blood also involves unavoidable higher toxicity to healthy tissues. Therefore, the half-life of the radionuclide should be compatible with the plasma half-life of the vector to ensure a sufficient high tumor/background ratio. One should note that the selectivity for radiation damage to malignant tissue is potentially higher for longer-lived radionuclides, which is beneficial in a therapeutic setting. In this respect, the short biological half-life of  $^{213}\text{Bi}$  is a disadvantage when combined with a carrier molecule with a long plasma half-life. Accumulation of such a carrier in the tumor tissue requires more time than the decay time of  $^{213}\text{Bi}$  (Fig. 7). In contrast,  $^{213}\text{Bi}$  is a much better match with vector molecules that have a short biological half-life such as some small molecules, several peptides, and antibody fragments (including nanobodies). These molecules accumulate rapidly in the tumor tissue, and therefore allow  $^{213}\text{Bi}$  to deposit its dose to the tumor before it is fully decayed (Fig. 7). The TAT studies with  $^{213}\text{Bi}$ -PSMA-617 in a patient with metastasized castration-resistant prostate cancer that was refractory to  $^{177}\text{Lu}$ -radiotherapy illustrates the potential of the combination of  $^{213}\text{Bi}$  with a vector molecule

with short biological half-life [88]. Further, an *in vitro* and *in vivo* preclinical studies with a  $^{213}\text{Bi}$ -labeled nanobody for TAT showed promising results (see table 3) [5].

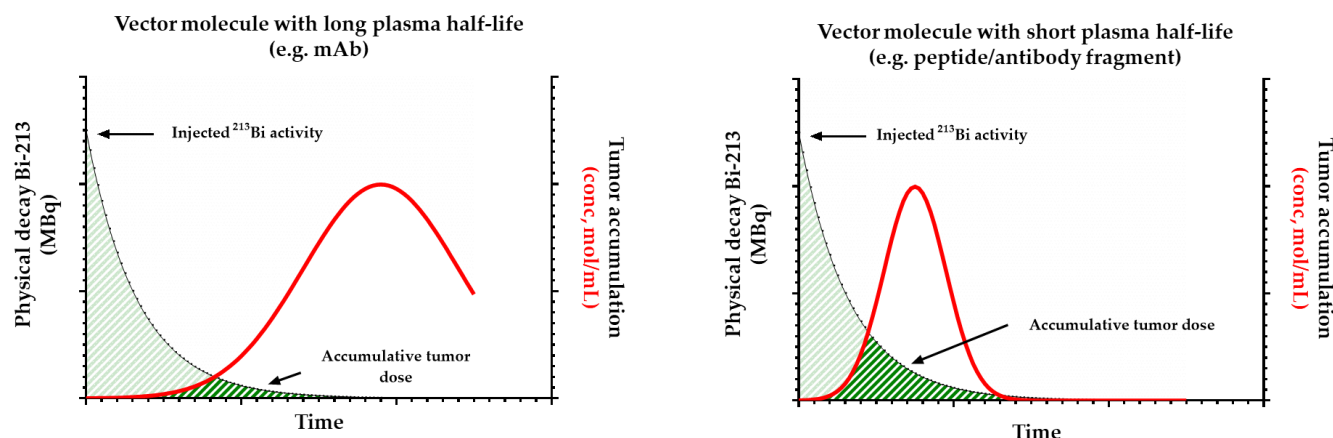


Figure 7. Accumulative tumor dose of a vector molecule with long and short biological half-life, respectively, in combination with the short-lived therapeutic radionuclide  $^{213}\text{Bi}$ .

Although carriers with a short plasma half-life are preferred for  $^{213}\text{Bi}$ , several combinations with slow kinetics carriers have been reported. One way to bypass the kinetic incompatibility is limiting its use to local therapy only. Locoregional delivery of  $^{213}\text{Bi}$ -radiopharmaceuticals compared to systematic administration has the potential to significantly increase efficacy, while minimizing systemic toxicity to non-targeted tissues. A disadvantage is that it is no longer a systemic treatment and that not all metastasis will be treated, except if after locoregional injection there is substantial spill-over to the systemic circulation (e.g. injection in the hepatic artery). With locoregional delivery, the short-lived radionuclide  $^{213}\text{Bi}$  can be combined with vector molecules with a long biological half-life such as mAbs as only high binding affinity to the target is important and not the pharmacokinetic properties of the radiopharmaceutical.

Pretargeted radiotherapy is another approach to combine a vector with long plasma half-life with a radionuclide with a short half-life such as  $^{213}\text{Bi}$  [89]. First, a tumor-accumulating vector molecule carrying a tag is administered systemically. Once accumulated at the target sites and largely cleared from the blood, a fast clearing radiolabeled agent that rapidly recognizes the tag of the tumor-bound vector *in vivo* is injected. Upon encountering the targeting vector, ligation will take place between the two molecules which leads to the *in vivo* formation of the final radioconjugate, resulting to specific irradiation of target tissue and low radiation burden of healthy tissue.

In the following two chapters non-clinical and clinical experiences with  $^{213}\text{Bi}$ -labeled probes will be discussed, organized by vector molecule.

## 6. Preclinical TAT studies with $^{213}\text{Bi}$ -labeled probes

### 6.1 Biomolecules

#### 6.1.1 Antibodies

Monoclonal antibodies (mAbs), with their impeccable affinity for tumor antigens, have become powerful tools in the diagnosis and treatment of cancer, particularly when combined with therapeutic agents such as radionuclides and cytotoxic drugs, thanks to advances in hybridoma technology in the 1980s [90,91]. A mAb has the potential to bind antigen epitopes with high affinity, including tumor-related antigens and are interesting vector molecules for TRNT because of high tumor accumulation (Fig. 6) [4]. A variety of preclinical investigations have been conducted using mAbs labeled with  $^{213}\text{Bi}$  as radio-metal (Table 3).

TRNT performed with 3.7 MBq of  $^{213}\text{Bi}$ -labeled 9E7.4 anti-CD138 mAb increased median survival to 80 days compared to 37 days for the untreated control and resulted in 45% cure in a multiple myeloma mice model.  $\beta$ -TRNT performed with 18.5 MBq of  $^{177}\text{Lu}$ -labeled 9E7.4 mAb was well tolerated and increased mouse survival significantly (54 vs. 37 days in the control group); however, the authors reported that no mice were cured with this treatment [92].

Another study has shown that fractionated intravesical TRNT with  $^{213}\text{Bi}$ -anti-EGFR-mAb is a promising approach in advanced bladder carcinoma. Therapeutic efficacy was evaluated via overall survival and toxicity toward normal urothelium by histopathological analysis. Mice without treatment and those treated with the native anti-EGFR-mAb showed median survivals of 65.4 and 57.6 d, respectively. After fractionated treatment with 0.93 MBq,  $^{213}\text{Bi}$ -anti-EGFR-mAb animals lived for an average of 141.5 d, with 33% survival for at least 268 d. The animals survived for an average of 131.8 d after fractionated treatment with 0.46 MBq  $^{213}\text{Bi}$ -anti-EGFR-mAb, with 30% survival for more than 300 d. Only the control group and the group treated twice with 0.93 MBq of  $^{213}\text{Bi}$ -anti-EGFR-mAb showed significant differences. Even after treatment with 3.7 MBq of  $^{213}\text{Bi}$ -anti-EGFR-mAb, no toxic side effects on the normal urothelium were observed. [93].

### 6.1.2 Antibody fragments

Recent advances in bioengineering have led to the development of antibody fragments such as Fab (50 kDa),  $\text{F(ab')}_2$  (110kDa), 25-kDa single-chain Fv (scFv), diabodies (55 kDa), nanobodies (15kDa) and minibodies (80 kDa) without affecting their affinity and specificity [94]. Smaller mAb derivatives are transported more rapidly to the tumor site and can penetrate the tumor more effectively. Because of their smaller size and lack of an Fc region, they are swiftly cleared from circulation, resulting in rapid tumor uptake and high tumor-to-background ratios (Fig. 6). Successful conjugation of  $^{213}\text{Bi}$  to anti-HER2 C6.5 scFv and diabody molecules have been reported. However, there was no tumor-specific therapeutic effect, which was most likely due to the *in vivo* instability of the scFv and diabody molecules. The physical half-life of  $^{213}\text{Bi}$ , 45.6 min, was found to be too short for the systemically administered diabody to directly localize in the developed solid tumor [95].

For the first time, a  $^{213}\text{Bi}$ -labeled HER2-sdAb nanobody was successfully produced and characterized *in vitro* and *in vivo* in a preclinical setting.  $^{213}\text{Bi}$ -DTPA-2Rs15d sdAb exhibited high *in vivo* stability and specific accumulation in target tissue after systemic i.v. administration in mice. When administered in therapeutic doses,  $^{213}\text{Bi}$ -DTPA-2Rs15d sdAb increased the median survival of mice (80 d compared to 56 d in the control group, particularly when used in combination with trastuzumab (140 d). These findings suggest that  $^{213}\text{Bi}$ -DTPA-sdAb could be used as a new radioconjugate for TAT, both alone and in combination with trastuzumab, to treat HER2<sup>+</sup> metastatic cancer. Also, the rapid accumulation (15 min) of  $^{213}\text{Bi}$ -labeled 2Rs15d sdAb in HER2-expressing tumors demonstrates that sdAbs are promising vector molecules in combination with the short-lived  $^{213}\text{Bi}$  [5].

## 6.2 Small molecules

### 6.2.1 Peptides

Peptides have been used extensively in nuclear medicine for peptide receptor radionuclide therapy (PRRT). In the randomized NETTER-1 clinical trial, treatment with  $^{177}\text{Lu}$ -DOTATATE resulted in markedly longer progression-free survival and a significantly higher response rate than high-dose octreotide LAR among patients with advanced mid-gut neuroendocrine tumors [96]. Peptides are designed by rational methods with high specificity and selectivity to bind to its target of interest. Due to their ease of synthesis using chemical or molecular biological techniques, peptide sequences can also be easily modified [97]. Oncogenic protein sequences, structures, and pattern interactions are all readily accessible, allowing peptides to be engineered specifically for TAT. Peptides have several important advantages over proteins or antibodies as vector molecule for TRNT:

they are small, mostly stable, easy to synthesize, they can be modified to further increase the metabolic stability and it is straightforward to attach a bifunctional chelator allowing radiolabeling. Furthermore, they are typically less immunogenic than recombinant antibodies or proteins [98].

An *in vitro* comparison of  $^{213}\text{Bi}$ - and  $^{177}\text{Lu}$ -radiation for PRRT has been performed. Absorbed doses up to 7 Gy were obtained by 5.2 MBq  $^{213}\text{Bi}$ -DOTATATE, and majority of the dose was caused by  $\alpha$ -particle radiation. The cell survival of BON or CA20948 cells after exposure to  $^{213}\text{Bi}$ -DTPA and  $^{213}\text{Bi}$ -DOTATATE showed a linear-exponential relationship with the absorbed dose, confirming the strong LET character of  $^{213}\text{Bi}$ . CA20948 demonstrated the standard curvature of the linear-quadratic model after exposure to  $^{177}\text{Lu}$ -DOTATATE and the reference  $^{137}\text{Cs}$  irradiation. 10% CA20948 cell survival was achieved at 3 Gy with  $^{213}\text{Bi}$ -DOTATATE, which is six times less than the 18 Gy needed for  $^{177}\text{Lu}$ -DOTATATE and also less than the 5 Gy required after  $^{137}\text{Cs}$  external exposure. [65].

**Table 3,** Overview of some preclinical studies with  $^{213}\text{Bi}$

Bioconjugate	Key findings	Cancer type	Reference
$^{213}\text{Bi}$ -anti-EGFR-mAb	The animals survived for an average of 131.8 d after fractionated treatment with 0.46 MBq $^{213}\text{Bi}$ -anti-EGFR-mAb, with 30% remaining for more than 300 d. Even after treatment with 3.7 MBq of $^{213}\text{Bi}$ -anti-EGFR-mAb, no toxic side effects on normal urothelium were observed.	Human bladder carcinoma	[93]
$^{213}\text{Bi}$ -69-11 antibody	Antibody 69-11 localized significantly in pancreatic ductal adenocarcinoma cancer (PDAC) xenografts in mice <i>in vivo</i> and <i>ex vivo</i> . TAT of PDAC xenografts with $^{213}\text{Bi}$ -69-11 was effective, safe, and CETN1-specific.	Pancreatic cancer	[15]
$^{213}\text{Bi}$ -h8C3 antibody	Treatments with anti-PD-1 antibody alone had a modest impact on tumor size, while the combination therapy with $^{213}\text{Bi}$ -h8C3 resulted in a substantial slowing of tumor development, and improved animal survival.	Melanoma	[99]
$^{213}\text{Bi}$ -8C3 or $^{213}\text{Bi}$ -6D2 antibody	Antibody binding to melanin was shown to be dependent on both charge and hydrophobic interactions, and <i>in vivo</i> evidence supports the development of 8C3 IgG as a radio-immunotherapy reagent for metastatic melanoma.	Melanoma	[100]
$^{213}\text{Bi}$ -DOTATATE	10% Cell survival of CA20948 was reached at 3 Gy with $^{213}\text{Bi}$ -DOTATATE, a factor six lower than the 18 Gy found for $^{177}\text{Lu}$ -DOTATATE and below the 5 Gy after $^{137}\text{Cs}$ external exposure.	Pancreatic cancer	[65]
$^{213}\text{Bi}$ -IMP288-mAb	$^{213}\text{Bi}$ -IMP288 cleared from the bloodstream rapidly; blood levels were $0.44 \pm 0.28\%$ ID/g 30 min after injection. Except for the kidneys, where uptake was $1.8 \pm 1.1\%$ ID/g 30 min after injection, uptake in normal tissues was poor.	Colon cancer	[6]

<b><sup>213</sup>Bi-MX35-mAb</b>	The tumor-free fraction in animals given 3 MBq/mL of <sup>213</sup> Bi-MX35 was 0.55, while it was 0.78 in animals given 9 MBq/mL of <sup>213</sup> Bi-MX35. The tumor-free fraction in the control group treated with unlabeled MX35 was 0.15. There was no significant drop in white blood cell counts or weight loss.	Ovarian cancer	[101]
<b><sup>213</sup>Bi-DTPA-PAN-622-mAb</b>	A pilot therapy study with <sup>213</sup> Bi-DTPA-PAN-622 demonstrated a significant effect on the primary tumor.	Breast cancer	[102]
<b><sup>213</sup>Bi-Anti-hCD138 Antibody</b>	TAT of 7.4 MBq and 11.1 MBq significantly improved survival ( $p = 0.0303$ and $p = 0.0070$ , respectively), whereas HIPEC and HIPEC + TAT treatments did not significantly ameliorate survival as compared to the control group.	Ovarian cancer	[103]
<b><sup>213</sup>Bi-DOTA-9E7.4-mAb</b>	TAT with 3.7 MBq of <sup>213</sup> Bi-labeled 9E7.4 anti-CD138 mAb increased median survival to 80 d compared to 37 days in the untreated control group and resulted in effected cure in 45 % of the animals.	Multiple myeloma (MM)	[92]
<b><sup>213</sup>Bi-anti-EGFR-mAb</b>	Treatment with <sup>213</sup> Bi-anti-EGFR-mAb resulted in an effective induction of cell death in EJ28Luc and LN18 cells.	Bladder carcinoma	[104]
<b><sup>213</sup>Bi-DTPA-anti-CD138-mAb</b>	The combined treatment resulted in significant tumor growth suppression and improved survival in the animals	MM	[105]
<b><sup>213</sup>Bi-DTPA-anti-CD38-MAb</b>	Treatment with <sup>213</sup> Bi-anti-CD38-mAb suppressed tumor growth in myeloma xenografts by inducing apoptosis in tumor tissue and significantly extended survival relative to controls.	MM	[106]
<b><sup>213</sup>Bi-DTPA-Cetuximab</b>	<sup>213</sup> Bi-cetuximab was found to be significantly more effective in the BRCA-1-mutated triple negative breast cancer (TNBC) cell line HCC1937 than BRCA-1-competent TNBC cell MDA-MB-231. siRNA knockdown of BRCA-1 or DNA-dependent protein kinase, catalytic subunit (DNA-PKcs), a key gene in non-homologous end-joining DSB repair pathway, also sensitized TNBC cells to <sup>213</sup> Bi-cetuximab.	Breast cancer	[107]
<b><sup>213</sup>Bi-DTPA-anti-CD20-mAb</b>	In CD20-expressing sensitive as well as chemoresistant, beta-radiation resistant, and gamma-radiation resistant NHL cells, <sup>213</sup> Bi-anti-CD20 induced apoptosis, activated caspase-3, caspase-2, and caspase-9, and cleaved PARP.	Non-Hodgkin lymphoma	[108]
<b><sup>213</sup>Bi-DOTA-biotin</b>	80% and 20% of mice treated with anti-CD45 Ab-SA conjugate followed by	Myeloid leukaemia	[109]

	800Ci of <sup>213</sup> Bi- or <sup>90</sup> Y-DOTA-biotin survived leukemia-free for more than 100 d with limited toxicity, respectively.		
<sup>213</sup> Bi-DTPA-C595-mAb and <sup>213</sup> Bi-DTPA-PAI2-mAb	After 16 weeks, systemic injections of <sup>213</sup> Bi-conjugate at doses of 111, 222, and 333 MBq/kg induced significant tumor growth delay in a dose-dependent manner, compared to the non-specific control at 333 MBq/kg.	Pancreatic cancer	[110]
<sup>213</sup> Bi-DOTA-biotin	Mice injected with anti-CD20 PTRNT or 22.2 MBq <sup>213</sup> Bi-DOTA-biotin had significantly slower tumor growth than controls (mean tumor volume 0.01 ± 0.02 vs. 203.38 ± 83.03 mm <sup>3</sup> after 19 days, respectively).	Non-Hodgkin lymphoma	[111]
<sup>213</sup> Bi-DTPA-7.16.4-mAb	In the same animal model, <sup>213</sup> Bi radio-labeled immunoliposomes were successful in treating early-stage micrometastases, with median survival times comparable to those obtained with antibody-mediated <sup>213</sup> Bi delivery.	Breast cancer	[112]
<sup>213</sup> Bi-DTPA-HuCC49ΔCH2	The median survival time after treatment with <sup>213</sup> Bi-HuCC49ΔCH2 was 45 days, which was equivalent to the median survival time after treatment with <sup>213</sup> Bi-trastuzumab.	Colon carcinoma	[78]
<sup>213</sup> Bi ( <sup>213</sup> Bi-DTPA-[F3] <sub>2</sub> )	Except for the kidneys, where <sup>213</sup> Bi-DTPA-[F3] <sub>2</sub> was present due to renal excretion, <sup>213</sup> Bi-DTPA-[F3] <sub>2</sub> accumulated significantly in tumors, but only low activities were found in control organs.	Peritoneal carcinomatosis	[113]
<sup>213</sup> Bi-DTPA-2Rs15d sdAb	Median survival significantly increased when <sup>213</sup> Bi-DTPA-2Rs15d was given alone or in combination with trastuzumab.	Ovarian cancer	[5]
<sup>213</sup> Bi-DTPA-PAI2-mAb	At 2 d and 2 weeks after cell inoculation, no lymphatic cancer spread was observed in the 222 MBq/kg <sup>213</sup> Bi-DTPA-PAI2-mAb treated class.	Prostate cancer	[114]

Important progress has been made in the production and application of <sup>213</sup>Bi-optimized vehicles so far. Despite the promising preliminary results, there is still much room for improvement, especially in the development of new coupling chemistries and the elucidation and optimization of in vivo biodistribution.

7. Clinical TAT studies with <sup>213</sup>Bi-labeled radiopharmaceuticals

It is suggested that TAT is ideally suited for hematologic malignancies due to the easy accessibility of malignant cells in blood, bone marrow, lymph node sand spleen as well as their typical high radiosensitivity [40,79]. The majority of clinical trials for hematologic malignancies using α-particle therapy have focused on acute myeloid leukemia (AML) [80,81]. Nonetheless, preclinical studies have shown activity against other cancer types, including non-Hodgkin's lymphoma and multiple myeloma [108,115].

To date,  $^{213}\text{Bi}$ -labeled radiopharmaceuticals has been used to treat more than 200 patients for leukemia, lymphoma, melanoma, bladder cancer, glioma, and neuroendocrine tumors [7]. The two main approaches currently used for the administration of this radiopharmaceutical are locoregional- and systemic administration.

### 7.1 Locoregional administration

#### 7.1.1 Intravesical TRNT

A locoregional pilot study to evaluate the feasibility, tolerability and efficacy of  $^{213}\text{Bi}$ -anti-EGFR mAb treatment in patients with *Bacillus Calmette-Guerin* (BCG) refractory carcinoma *in situ* (CIS) has been performed [13]. A single intravesical instillation (or two instillations) of 366–821 MBq of  $^{213}\text{Bi}$ -anti-EGFR immunoconjugate (with molar activities in the range of 0.37–0.82 GBq/mg) was tolerated without any adverse effects. Four patients showed a complete response, i.e. no visible CIS, eight weeks after the first or second treatment. Three of the four patients were still tumor-free at the time of the publication, i.e. three months after the second treatment and 30 and 44 months after the first treatment. However, since this was a pilot studies the authors concluded that additional studies are required to confirm this therapeutic outcome [13].

#### 7.1.2 Intracerebral Substance-P PRRT

Interest in PRRT has steadily grown because of the advantages of targeting cellular receptors *in vivo* with highly tumor-specific targeting and high tumoral activity concentration. Unparalleled attempts to develop radiolabeled receptor-binding somatostatin analogues for the treatment of neuroendocrine tumors have occurred in recent decades, and these efforts have facilitated the evolution of PRRT and paved the way for the development of other receptor-targeting peptides. [96,116–118]. The highest number of patients treated with locoregional administration of  $^{213}\text{Bi}$  has been gathered with the treatment of grade II to IV glioma with radiolabeled DOTA-Substance P analog (substance-P binds to GPCR neurokinin type 1 receptor). This radiopharmaceutical has a relatively low molecular weight (1.8 kDa) and can therefore overcome the blood-brain barrier; however, its short plasma half-life presented a challenge to researchers. In a clinical study,  $^{213}\text{Bi}$ -Substance P was administered locoregionally into the tumor or tumor cavity via an implanted catheter. Patients were treated with up to 14.1 GBq  $^{213}\text{Bi}$ -Substance P, administered in up to eight treatment cycles at two-month intervals. No severe side effects were recorded. The median survival time from the start of  $^{213}\text{Bi}$ -DOTA-SP was 7.5 months. Several patients showed complete remissions and no recurrence was observed up to 20 years after the end of therapy. A subgroup analysis indicated prolonged survival times for grade IV patients in comparison with standard treatments [84]. These data should encourage future randomized controlled trials.

#### 7.1.3 Intra lesional melanoma TRNT

Intralesional therapy injection of a high concentration of a drug directly into skin lesions without significant systemic absorption, is also becoming increasingly popular. The rationale for this technique is the establishment of a subepidermal depot which bypasses the superficial barrier zone.

For e.g. intra lesional melanoma TRNT with  $^{213}\text{Bi}$  conjugated to the benign tumor targeting vector 9.2.27 has been studied. Sixteen melanoma patients positive to the monoclonal antibody 9.2.27 were recruited.  $\alpha$ -immunoconjugate activities from 5.5 to 50 MBq injected into lesions of different sizes resulted in massive cell death, as observed by the presence of tumor debris. The  $\alpha$ -immunoconjugate was very good at providing a high dose to the tumor while sparing the surrounding tissues. Blood proteins and electrolytes did not display any major changes. [119].

### 7.2 Systemic administration

### 7.2.1 Acute myeloid Leukemia TRNT

mAb-TAT uses antibodies against a tumor-associated antigen labeled with a  $\alpha$ -emitting radionuclide to deliver a lethal dose of radiation to tumor cells. Table 4 summarizes the current state of clinical investigation of  $^{213}\text{Bi}$ -radiopharmaceuticals.

An initial phase I study conducted in 18 patients with relapsed or refractory Acute Myeloid Leukemia (AML) demonstrated the safety and antitumor effects of  $^{213}\text{Bi}$ -lintuzumab. Subsequently,  $^{213}\text{Bi}$ -lintuzumab produced remissions in AML patients after partial cytoreduction with cytarabine in phase I/II trial [80,81]. The short half-life of  $^{213}\text{Bi}$  and need for an onsite generator presented a major obstacle to the wide-spread use of mAb-TAT with  $^{213}\text{Bi}$ . Therefore, a second-generation construct was developed using  $^{225}\text{Ac}$  which was directly conjugated to the antibody. A phase I trial demonstrated that a single infusion of  $^{225}\text{Ac}$ -lintuzumab could be given safely at doses up to 111 kBq/kg with anti-leukemic activity across all activity levels studied. In a second phase I study, 28% of older patients with untreated AML had objective responses after receiving fractionated  $^{225}\text{Ac}$ -lintuzumab and low-dose cytarabine [120,121].

### 7.2.2 SSTR PRRT

The only  $^{213}\text{Bi}$  PRRT study so far was performed by Kratochwil C. et al. in 2014. Eight patients with multi-resistant neuroendocrine tumors refractory to therapy with beta emitter labeled  $^{90}\text{Y}$ -/ $^{177}\text{Lu}$ -DOTATOC were treated with  $^{213}\text{Bi}$ -DOTATOC. Seven of them underwent intra-arterial injection into the hepatic artery, which results in an enriched exposure of the liver metastases but also allows systemic targeting. Even though the patients presented were in an advanced disease setting and had developed resistance against therapy with beta emitting  $^{90}\text{Y}$ -/ $^{177}\text{Lu}$ -DOTATOC,  $^{213}\text{Bi}$ -DOTATOC resulted in a considerable number of long-lasting antitumor responses, including one complete remission (Fig. 8) [16].

### 7.2.3 $^{213}\text{Bi}$ -PSMA

PSMA accounts for about 95% of the extracellular domain and provides a molecular target for small molecules, antibodies, and antibody fragments [122]. A first-in-human treatment with  $^{213}\text{Bi}$ -PSMA-617 was performed in a patient with mCRPC (metastatic castration-resistant prostate cancer) that was progressive under conventional therapy. The patient was treated with two cycles of  $^{213}\text{Bi}$ -PSMA-617 with a cumulative activity of 592 MBq. Restaging with  $^{68}\text{Ga}$ -PSMA PET/CT after 11 months showed an outstanding molecular imaging response. This patient also exhibited a biochemical response (decrease in prostate-specific antigen levels from 237  $\mu\text{g/L}$  to 43  $\mu\text{g/L}$ ) [88].

**Table 4,** Overview of Clinical Studies with  $^{213}\text{Bi}$ -labeled Ligands

Cancer type	Radioligand	Patients	Reference
Leukemia	$^{213}\text{Bi}$ -anti-CD33-mAb (SA)	49	[80,81]
Melanoma	$^{213}\text{Bi}$ -anti-MCSP-mAb (SA)	54	[123–125]
Glioma	$^{213}\text{Bi}$ -Substance P (SA)	68	[14,83–85]
Bladder cancer	$^{213}\text{Bi}$ -anti-EGFR-mAb (LR)	12	[13]
Neuroendocrine tumor	$^{213}\text{Bi}$ -DOTATOC (SA)	25	[16]
mCRPCa	$^{213}\text{Bi}$ -PSMA	1	[88]

SA = systematic administration, LR = locoregional administration

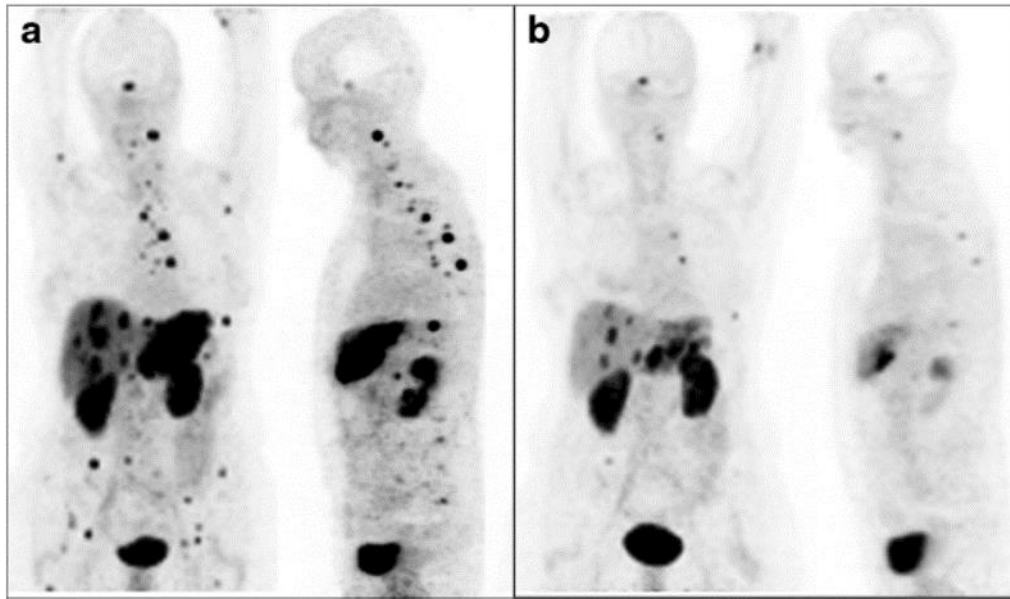


Figure 8,  $^{68}\text{Ga}$ -DOTATOC-PET image of a patient (a) after treatment with  $^{90}\text{Y}/^{177}\text{Lu}$ -DOTATOC (b) after systematic administration of a total cumulative dose of 10.5 GBq of  $^{213}\text{Bi}$ -DOTATOC [16]. Image was adapted with permission from C. Kratochwil et. al., 2014.

## 8. Future perspectives of $^{213}\text{Bi}$ -TAT

The recent data on the remarkable therapeutic efficacy of  $^{213}\text{Bi}$ -bioconjugates for cancer therapy have significantly ignited interest in the clinical application of TAT. The implementation of  $^{213}\text{Bi}$ -bioconjugates does not only offer an auspicious therapeutic option for cancer treatment, but also strongly underlines an important potential of the concept of TAT. The clinical studies data from  $^{213}\text{Bi}$ -DOTATOC and  $^{213}\text{Bi}$ -PSMA-617 suggest that therapy with  $\alpha$ -emitters is likely to prevent resistance to therapy with conventional drugs and also with  $\beta$ -emitters and could provide a useful additional treatment option to patients that were progressive under conventional treatments. To successfully translate  $^{213}\text{Bi}$ -bioconjugate probes from bench-to-bedside one needs to consider the half-life of  $^{213}\text{Bi}$  (46 min), which should match the tumor and plasma kinetics of the vector molecule. Evidently, a therapeutic agent which dispels most of its energy before reaching its target will cause more harm than good. Low molecular weight peptide ligands and antibody fragments labeled with  $^{213}\text{Bi}$  are for this reason promising due to their favorable fast pharmacokinetics.

Also, cancer-associated fibroblasts (CAF), which are highly expressed in the stroma of most tumor entities, is an emerging area for consideration. CAFs, in contrast with normal fibroblasts, overexpress fibroblast activation protein  $\alpha$  (FAP). Novel radioprobes, both for diagnostic and therapeutic applications, were designed and are based on FAP inhibitors (FAPI) as vector molecule (e.g.  $^{68}\text{Ga}$ -DOTA-FAPI-46). FAPI PET images are characterized by rapid kinetics, very low background activity (no uptake in brain, muscle, brown fat, bowel,...) and high tumor-to-background contrast. The fast pharmacokinetics of FAPI vector molecules might be an ideal match with the short physical half-life of  $^{213}\text{Bi}$  [126–129]. Hence, this will be an interesting area to explore for future  $^{213}\text{Bi}$  radiopharmaceutical development.

For  $^{213}\text{Bi}$  chelation chemistry, although at first sight there are decent number of ligands that have been used to synthesize its radio-complexes, closer inspection reveals these “gold standard” ligands such as DOTA might not be ideal for clinical application. The chelator should clearly match with the chemical properties of  $^{213}\text{Bi}$ . Consideration of thermodynamic stability should be balanced with the formation kinetics of such species. This is particularly important for the practicalities of the synthesis of radiopharmaceuticals. NETA and DEPA derivatives have so far demonstrated to be an ideal match for  $^{213}\text{Bi}$ .

However, this potential of NETA and DEPA for use in  $^{213}\text{Bi}$  radiopharmaceuticals requires further investigation before it can be translated to a clinical setting.

Another area to consider is *in vivo* kidney toxicity, due to kidney uptake and retention of  $^{213}\text{Bi}$ -radioprobes. The mechanisms responsible for unwanted kidney uptake and retention are well explored. Radioconjugates with a molecular weight of less than 60 kDa (Fig. 6) are filtered through the glomerulus, reabsorbed, and transported to the lysosomal compartment. The long residence time of radionuclides in the kidney decreases imaging sensitivity and causes a high radiation burden for the kidneys. This can lead to tubular necrosis, and limits the therapeutic dose, especially when using the short-lived radionuclide  $^{213}\text{Bi}$ . Several strategies have been explored to mitigate the toxic aspect of  $^{213}\text{Bi}$ -labeled radioprobes during cancer treatment [5,66,130,131] and some of these approaches have been approved for clinical applications. The co-infusion of lysine or the plasma expander Gelofusine® with  $^{213}\text{Bi}$ -bioconjugates during TAT has been reported to have a threefold reduction in the kidney uptake and retention [66,132]. Another promising approach could be that  $^{213}\text{Bi}$ -radioprobes will be developed with a cleavable linker, positioned between the Bi-chelator complex and vector molecule, that is recognized specifically by renal brush border membrane enzymes, so that the radionuclides are excreted more efficiently towards the bladder instead of being retained in the kidneys.

A study has demonstrated that derivatives of [ $^{68}\text{Ga}$ ]Ga-DOTA-AmBz-MVK-OH could be cleaved specifically by neutral endopeptidase (NEP), and therefore, the amino acids linker MVK could reduce kidney uptake of radiolabeled DOTA-conjugated peptides and peptidomimetics [133]. These findings would allow to develop radiometal-based radiopharmaceuticals with clinically relevant lower renal radioactivity levels [134].

To conclude, TAT using  $^{213}\text{Bi}$  has demonstrated interesting results preclinically and clinically. The limitation is that  $^{213}\text{Bi}$  radionuclide has relatively a shorter half-life (46 min). However, it can be made available to the hospitals over a minimum of a 10-day period when using an  $^{225}\text{Ac}/^{213}\text{Bi}$  generator. Another advantage of  $^{213}\text{Bi}$  is that the short half-life could provide rapid release of lethal radiation after injection and is an ideal match for vector molecules with fast plasma clearance, fast tumor targeting but also limited tumoral retention.

**Author Contributions:** Writing – original draft preparation, S. A. and F.C; writing – review and editing, S.A., I.C., C.M.D, T.C, A.R.B, G.B., M.O. and F.C.

**Funding:** SCK CEN Academy is gratefully acknowledged. Frederik Cleeren is a Postdoctoral Fellow of FWO (12R3119N). Christophe M. Deroose is a Senior Clinical Investigator at the FWO.

**Conflicts of Interest:** The authors declare no conflict of interest.

## References

1. Vermeulen K, Vandamme M, Bormans G, Cleeren F. Design and Challenges of Radiopharmaceuticals. Vol. 49, Semin Nucl Med. W.B. Saunders; 2019. p. 339–56.
2. Kostelnik TI, Orvig C. Radioactive Main Group and Rare Earth Metals for Imaging and Therapy. Chem Rev. 2018;2(119):902–56.
3. Price EW, Orvig C. Matching chelators to radiometals for radiopharmaceuticals. Chem Soc Rev. 2014 Jan 7;43(1):260–90.
4. Dekempeneer Y, Keyaerts M, Krasniqi A, Puttemans J, Muyldermans S, Lahoutte T, et al. Targeted alpha therapy using short-lived alpha-particles and the promise of nanobodies as targeting vehicle. Expert Opin Biol Ther. 2016 Aug 2;16(8):1035–47.
5. Dekempeneer Y, Caveliers V, Ooms M, Maertens D, Gysemans M, Lahoutte T, et al. The therapeutic efficacy of <sup>213</sup>Bi-labeled sdAbs in a preclinical model of ovarian cancer. Mol Pharm. 2020 Sep 8;17(9):3553–66.
6. Heskamp S, Hernandez R, Molkenboer-Kuenen JDM, Essler M, Bruchertseifer F, Morgenstern A, et al.  $\alpha$ -Versus  $\beta$ -Emitting radionuclides for pretargeted radioimmunotherapy of carcinoembryonic antigen-expressing human colon cancer xenografts. J Nucl Med. 2017 Jun 1;58(6):926–33.
7. Bruchertseifer F, Kellerbauer A, Malmbeck R, Morgenstern A. Targeted alpha therapy with bismuth-213 and actinium-225: Meeting future demand. J Label Compd Rad. 2019 Sep 1;62(11):794–802.
8. Beyls C, Haustermans K, Deroose CM, Pans S, Vanbeckevoort D, Verslype C, et al. Could Autoimmune Disease Contribute to the Abscopal Effect in Metastatic Hepatocellular Carcinoma? Hepatology. 2020 Sep 1;72(3):1152–4.
9. Gill MR, Vallis KA. Transition metal compounds as cancer radiosensitizers. Chem Soc Rev. 2019 Jan 21;48(2):540–57.
10. Lacoeuille F, Arlicot N, Faivre-Chauvet A. Targeted alpha and beta radiotherapy: An overview of radiopharmaceutical and clinical aspects. Med Nucl. 2018;42(1):32–44.
11. Turner JH. Recent advances in theranostics and challenges for the future. Br J Radiol. 2018 Mar 29;91(1091):20170969.
12. Qaim SM. Theranostic radionuclides: recent advances in production methodologies. J Radioanal Nucl Chem. 2019 Dec 1;322(3):1257–66.
13. Autenrieth ME, Seidl C, Bruchertseifer F, Horn T, Kurtz F, Feurecker B, et al. Treatment of carcinoma in situ of the urinary bladder with an alpha-emitter immunoconjugate targeting the epidermal growth factor receptor: a pilot study. Eur J Nucl Med Mol I. 2018 Jul 1;45(8):1364–71.
14. Krolicki L, Bruchertseifer F, Kunikowska J, Koziara H, Królicki B, Jakuciński M, et al. Prolonged survival in secondary glioblastoma following local injection of targeted alpha therapy with <sup>213</sup>Bi-substance P analogue. Eur J Nucl Med Mol Imaging. 2018 Jul 30;45(9):1636–44.
15. Jiao R, Allen KJH, Malo ME, Helal M, Jiang Z, Smart K, et al. Evaluation of novel highly specific antibodies to cancer testis antigen Centrin-1 for radioimmunoimaging and radioimmunotherapy of pancreatic cancer. Cancer Med. 2019 Sep 1;8(11):5289–300.
16. Kratochwil C, Giesel FL, Bruchertseifer F, Mier W, Apostolidis C, Boll R, et al. <sup>213</sup>Bi-DOTATOC receptor-targeted alpha-radionuclide therapy induces remission in neuroendocrine tumours refractory to beta radiation: a first-in-human experience. Eur J Nucl Med Mol Imaging. 2014 Nov;41(11):2106–19.
17. Morgenstern A, Apostolidis C, Kratochwil C, Sathekge M, Krolicki L, Bruchertseifer F. An Overview of Targeted Alpha Therapy with <sup>225</sup>Actinium and <sup>213</sup>Bismuth. Curr Radiopharm. 2018 Sep 11;11(3):200–8.
18. Sgouros G, Roeske JC, McDevitt MR, Palm S, Allen BJ, Fisher DR, et al. MIRD pamphlet No. 22 (Abridged): Radiobiology and dosimetry of  $\alpha$ -particle emitters for targeted radionuclide therapy. J Nucl Med. 2010 Feb 1;51(2):311–28.
19. Morgenstern A, Bruchertseifer F, Apostolidis C. Targeted Alpha Therapy with <sup>213</sup>Bi. Curr Radiopharm. 2012 Oct 30;4(4):295–305.
20. Feurecker B, Tauber R, Knorr K, Heck M, Beheshti A, Seidl C, et al. Activity and Adverse Events of Actinium-225-PSMA-617 in Advanced Metastatic Castration-resistant Prostate Cancer After Failure of Lutetium-177-PSMA. Eur Urol Suppl. 2020 Mar 1;79(3):343–50.

21. Zacherl MJ, Gildehaus FJ, Mittlmeier L, Boening G, Gosewisch A, Wenter V, et al. First clinical results for PSMA targeted alpha therapy using  $^{225}\text{Ac}$ -PSMA-I&T in advanced mCRPC patients. *J Nucl Med*. 2020 Oct 2;jnumed.120:Abstract.
22. Kratochwil C, Bruchertseifer F, Rathke H, Bronzel M, Apostolidis C, Weichert W, et al. Targeted  $\alpha$ -therapy of metastatic castration-resistant prostate cancer with  $^{225}\text{Ac}$ -PSMA-617: Dosimetry estimate and empiric dose finding. *J Nucl Med*. 2017 Oct 1;58(10):1624–31.
23. Zielinska B, Apostolidis C, Bruchertseifer F, Morgenstern A. An improved method for the production of  $^{225}\text{Ac}$ - $^{213}\text{Bi}$  from  $^{229}\text{Th}$  for targeted alpha therapy. *Solvent Extr Ion Exch*. 2007 May;25(3):339–49.
24. Apostolidis C, Molinet R, Rasmussen G, Morgenstern A. Production of  $^{225}\text{Ac}$  from  $^{229}\text{Th}$  for targeted  $\alpha$  therapy. *Anal Chem*. 2005 Oct 1;77(19):6288–91.
25. Boden S, Vints K, Cagno S, Maertens D, Van Hecke K, Cardinaels T. Thorium-229 quantified in historical Thorium-228 capsules. *Appl Radiat Isot*. 2017 Feb 1;120:40–4.
26. Apostolidis C, Molinet R, McGinley J, Abbas K, Möllenbeck J, Morgenstern A. Cyclotron production of  $^{225}\text{Ac}$  for targeted alpha therapy. *Appl Radiat Isot*. 2005 Mar;62(3):383–7.
27. Morgenstern A, Abbas K, Bruchertseifer F, Apostolidis C. Production of Alpha Emitters for Targeted Alpha Therapy. *Curr Radiopharm*. 2008 Sep 1;1(3):135–43.
28. Nesteruk KP, Ramseyer L, Carzaniga TS, Braccini S. Measurement of the Beam Energy Distribution of a Medical Cyclotron with a Multi-Leaf Faraday Cup. *Instruments*. 2019 Jan 4;3(1):4.
29. Engle JW, Mashnik SG, Weidner JW, Wolfsberg LE, Fassbender ME, Jackman K, et al. Cross sections from proton irradiation of thorium at 800 MeV. *Phys Rev C*. 2013 May 28;88(1):014604.
30. Weidner JW, Mashnik SG, John KD, Hemez F, Ballard B, Bach H, et al. Proton-induced cross sections relevant to production of  $^{225}\text{Ac}$  and  $^{223}\text{Ra}$  in natural thorium targets below 200MeV. *Appl Radiat Isot*. 2012 Nov 1;70(11):2602–7.
31. Copping R, Mirzadeh S SD. Radium targets for the reactor production of alpha-emitting medical radioisotopes. In: *J Med Imag Radiat Sci*. Elsevier BV; 2019. p. S83.
32. Boll RA, Garland M, Mirzadeh S. Reactor production of thorium-229. In: *AIP Conf Proc*. AIP; 2005. p. 1674–5.
33. Melville G, Meriarty H, Metcalfe P, Knittel T, Allen BJ. Production of  $^{225}\text{Ac}$  for cancer therapy by photon-induced transmutation of  $^{226}\text{Ra}$ . *Appl Radiat Isot*. 2007 Sep;65(9):1014–22.
34. Robertson AKH, Ramogida CF, Schaffer P, Radchenko V. Development of  $^{225}\text{Ac}$  Radiopharmaceuticals: TRIUMF Perspectives and Experiences. *Curr Radiopharm*. 2018 Apr 18;11(3):156–72.
35. Grimm T, Grimm A, Peters W ZM. High-purity actinium-225 production from radium-226 using a superconducting electron linac. In: 11th International Symposium on Targeted-Alpha-Therapy, Ottawa, Canada. In: *J Med Imag Radiat Sci*. Elsevier BV; 2019. p. S12–3.
36. Maslov OD, Sabel'nikov A V., Dmitriev SN. Preparation of  $^{225}\text{Ac}$  by  $^{226}\text{Ra}(\gamma, n)$  photonuclear reaction on an electron accelerator, MT-25 microtron. *Radiochemistry*. 2006 Mar;48(2):195–7.
37. Morgenstern A, Bruchertseifer F, Apostolidis C. Bismuth-213 and Actinium-225 – Generator Performance and Evolving Therapeutic Applications of Two Generator-Derived Alpha-Emitting Radioisotopes. *Curr Radiopharm*. 2012 Jun 1;5(3):221–7.
38. Ma D, McDevitt MR, Finn RD, Scheinberg DA. Breakthrough of  $^{225}\text{Ac}$  and its radionuclide daughters from an  $^{225}\text{Ac}/^{213}\text{Bi}$  generator: Development of new methods, quantitative characterization, and implications for clinical use. *Appl Radiat Isot*. 2001;55(5):667–78.
39. Sinenko IL, Kalmykova TP, Likhoshesterova D V., Egorova B V., Zubenko AD, Vasiliev AN, et al.  $^{213}\text{Bi}$  production and complexation with new picolinate containing ligands. *J Radioanal Nucl Chem*. 2019 Aug 15;321(2):531–40.
40. Morgenstern A, Apostolidis C, Bruchertseifer F. Supply and Clinical Application of Actinium-. *Semin Nucl Med*. 2020;50(2):119–23.

41. Michael R. McDevitt, Ronald D. Finn, George Sgouros DM, David A. Scheinberg. An  $^{225}\text{Ac}$  /  $^{213}\text{Bi}$  generator system for therapeutic clinical applications: construction and operation. *Appl Radiat Isot.* 1999;50:895–904.
42. Mehring M. From molecules to bismuth oxide-based materials: Potential homo-and heterometallic precursors and model compounds. *Coord Chem Rev.* 251(7–8):974–1006.
43. Briand GG, Burford N. Bismuth Compounds and Preparations with Biological or Medicinal Relevance. *Chem Rev.* 1999 Sep;99(9):2601–58.
44. ANANTHAKRISHNAN S V. The electronic theory of valency. *Curr Sci.* 1946 Feb 1;15(3049):33–5.
45. Pyykkö P. Relativistic Effects in Structural Chemistry. *Chem Rev.* 1988 May 1;88(3):563–94.
46. Ershov BG, Akinshin MA, Gordeev A V., Sukhov NL. A pulse radiolysis study of the chloride complexes of Bi(II) and Bi(IV). *Int J Radiat Appl Instrumentation Part.* 1986;27(2):91–2.
47. Tooth B, Etschmann B, Pokrovski GS, Testemale D, Hazemann JL, Grundler P V., et al. Bismuth speciation in hydrothermal fluids: An X-ray absorption spectroscopy and solubility study. *Geochim Cosmochim Acta.* 2013;101:156–72.
48. Näslund J, Persson I, Sandström M. Solvation of the bismuth(III) ion by water, dimethyl sulfoxide, N,N'-dimethylpropyleneurea, and N,N-dimethylthioformamide. An EXAFS, large-angle X-ray scattering, and crystallographic structural study. *Inorg Chem.* 2000;39(18):4012–21.
49. Sun Hongzhe, Li H, Sadler PJ. The biological and medicinal chemistry of bismuth. *Chem Ber.* 1997;130(6):669–81.
50. Tooth B. The Hydrothermal Chemistry of Bismuth and The Liquid Bismuth Collector Model [Internet]. [Adelaide]: University of Adelaide; 2013 [cited 2021 Feb 19]. Available from: <https://digital.library.adelaide.edu.au/dspace/handle/2440/83112>
51. Pearson RG. Hard and soft acids and bases, HSAB, part I: Fundamental principles. *J Chem Ed.* 1968;45(9):581–7.
52. Li MX, Zhang LZ, Yang M, Niu JY, Zhou J. Synthesis, crystal structures, in vitro biological evaluation of zinc(II) and bismuth(III) complexes of 2-acetylpyrazine N(4)-phenylthiosemicarbazone. *Bioorganic Med Chem Lett.* 2012;22(7):2418–23.
53. Ferraz KSO, Silva NF, Da Silva JG, De Miranda LF, Romeiro CFD, Souza-Fagundes EM, et al. Investigation on the pharmacological profile of 2,6-diacetylpyridine bis(benzoylhydrazone) derivatives and their antimony(III) and bismuth(III) complexes. *Eur J Med Chem.* 2012;53(2):98–106.
54. Sadler PJ, Li H, Sun H. Coordination chemistry of metals in medicine: Target sites for bismuth. *Coord Chem Rev.* 1999 May 1;185–186:689–709.
55. Hancock RD, Baloyi J, Mashishi J. The Affinity of Bismuth ( rii ) for Nitrogen-donor Ligands. *J Chem Soc Dalt Trans.* 1993;5(3).
56. Guo Z, Sadler PJ. Metals in Medicine: Metal-based drugs. *Angew Chem Int Ed.* 1999;38:1512–31.
57. Dorso L, Bigot-Corbel E, Abadie J, Diab M, Gouard S, Bruchertseifer F, et al. Long-Term Toxicity of  $^{213}\text{Bi}$ -Labelled BSA in Mice. Xu B, editor. *PLoS One.* 2016 Mar 16;11(3):e0151330.
58. Garmestani K, Yao Z, Zhang M, Wong K, Park CW, Pastan I, et al. Synthesis and evaluation of a macrocyclic bifunctional chelating agent for use with bismuth radionuclides. *NUCL MED BIOL.* 2001 May 1;28(4):409–18.
59. Bomanji JB, Papathanasiou ND.  $^{111}\text{In}$ -DTPA0-octreotide (Octreoscan),  $^{131}\text{I}$ -MIBG and other agents for radionuclide therapy of NETs. *Eur J Nucl Med Mol Imaging.* 2012 Feb;39(Suppl 1:S112-25).
60. Rizzieri D. Zevalin® (ibritumomab tiuxetan): After more than a decade of treatment experience, what have we learned? *Crit Rev Oncol Hematol .* 2016 Sep 1;105:5–17.
61. Montavon G, Le Du A, Champion J, Rabung T, Morgenstern A. DTPA complexation of bismuth in human blood serum. *Dalt Trans.* 2012 Jul 28;41(28):8615–23.
62. Brechbiel MW, Gansow OA. Synthesis of C-functionalized trans-cyclohexyldiethylenetriaminepenta-acetic acids for labelling of monoclonal antibodies with the bismuth-212  $\alpha$ -particle emitter. *J Chem Soc, Perkin Trans 1.* 1992 Jan 1;0(9):1173–8.
63. Milenic DE, Roselli M, Mirzadeh S, Pippin CG, Gansow OA, Colcher D, et al. In Vivo evaluation of bismuth-labeled monoclonal antibody comparing DTPA-derived bifunctional chelates. *CANCER BIOTHER RADIO.* 2001;16(2):133–46.

- 
64. Camera L, Kinuya S, Garmestani K, Wu C, Brechbiel MW, Pai LH, et al. Evaluation of the Serum Stability and In Vivo Biodistribution of CHX-DTPA and Other Ligands for Yttrium Labeling of Monoclonal Antibodies. *J Nucl Med.* 1994;35(5):882–9.
  65. Chan HS, de Blois E, Morgenstern A, Bruchertseifer F, de Jong M, Breeman W, et al. In Vitro comparison of  $^{213}\text{Bi}$ - and  $^{177}\text{Lu}$ -radiation for peptide receptor radionuclide therapy. Xu B, editor. *PLoS One.* 2017 Jul 21;12(7):e0181473.
  66. Chan HS, Konijnenberg MW, Daniels T, Nysus M, Makvandi M, de Blois E, et al. Improved safety and efficacy of  $^{213}\text{Bi}$ -DOTATATE-targeted alpha therapy of somatostatin receptor-expressing neuroendocrine tumors in mice pre-treated with L-lysine. *EJNMMI Res.* 2016 Dec 21;6(1):83.
  67. Va Csajbó EÄ, Baranyai Z, Bányai I, Bru E, Ró J, Király B, et al. Equilibrium,  $^1\text{H}$  and  $^{13}\text{C}$  NMR Spectroscopy, and X-ray Diffraction Studies on the Complexes  $\text{Bi}(\text{DOTA})$ -and  $\text{Bi}(\text{DO3A-Bu})$ . *Inorg Chem.* 2003;7(42):2342–9.
  68. Šimeček J, Hermann P, Seidl C, Bruchertseifer F, Morgenstern A, Wester HJ, et al. Efficient formation of inert  $\text{Bi}$ - $^{213}\text{Bi}$  chelates by tetrakisphosphorus acid analogues of DOTA: towards improved alpha-therapeutics. *EJNMMI Res.* 2018 Aug 8;8(1):1–6.
  69. Lima LMP, Beyler M, Delgado R, Platas-Iglesias C, Tripier R. Investigating the Complexation of the  $\text{Pb}^{2+}/\text{Bi}^{3+}$  Pair with Dipicolinate Cyclen Ligands. *Inorg Chem.* 2015 Jul 20;54(14):7045–57.
  70. Lima LMP, Beyler M, Oukhatar F, Le Saec P, Faivre-Chauvet A, Platas-Iglesias C, et al.  $\text{H}_2\text{Me-d}^{202}\text{pa}$ : An attractive chelator with fast, stable and inert  $\text{natBi}^{3+}$  and  $^{213}\text{Bi}^{3+}$  complexation for potential  $\alpha$ -radioimmunotherapy applications. *Chem Comm.* 2014 Oct 21;50(82):12371–4.
  71. Chong HS, Song HA, Birch N, Le T, Lim S, Ma X. Efficient synthesis and evaluation of bimodal ligand NETA. *Bioorg Med Chem Lett.* 2008 Jun 1;18(11):3436–9.
  72. Song HA, Kang CS, Baidoo KE, Milenic DE, Chen Y, Dai A, et al. Efficient Bifunctional Decadentate Ligand 3p-C-DEPA for Targeted  $\alpha$ -Radioimmunotherapy Applications. *Bioconjug Chem.* 2011 Jun 15;22(6):1128–35.
  73. Chong HS, Milenic DE, Garmestani K, Brady ED, Arora H, Pfister C, et al. In vitro and in vivo evaluation of novel ligands for radioimmunotherapy. *Nucl Med Biol.* 2006 May 1;33(4):459–67.
  74. Chong HS, Song HA, Ma X, Milenic DE, Brady ED, Lim S, et al. Novel bimodal bifunctional ligands for radioimmunotherapy and targeted MRI. *Bioconjug Chem.* 2008 Jul;19(7):1439–47.
  75. Kang CS, Song HA, Milenic DE, Baidoo KE, Brechbiel MW, Chong HS. Preclinical evaluation of NETA-based bifunctional ligand for radioimmunotherapy applications using  $^{212}\text{Bi}$  and  $^{213}\text{Bi}$ : Radiolabeling, serum stability, and biodistribution and tumor uptake studies. *Nucl Med Biol.* 2013 Jul;40(5):600–5.
  76. Dadwal M, Kang CS, Song HA, Sun X, Dai A, Baidoo KE, et al. Synthesis and evaluation of a bifunctional chelate for development of  $\text{Bi}(\text{III})$ -labeled radioimmunoconjugates. *Bioorg Med Chem Lett.* 2011 Dec 15;21(24):7513–5.
  77. Chong HS, Lim S, Baidoo KE, Milenic DE, Ma X, Jia F, et al. Synthesis and biological evaluation of a novel decadentate ligand DEPA. *Bioorg Med Chem Lett.* 2008 Nov 1;18(21):5792–5.
  78. Milenic DE, Brady ED, Garmestani K, Albert PS, Abdulla A, Brechbiel MW. Improved efficacy of  $\alpha$ -particle-targeted radiation therapy: Dual targeting of human epidermal growth factor receptor-2 and tumor-associated glycoprotein 72. *Cancer.* 2010 Feb 15;116(SUPPL. 4):1059–66.
  79. Jurcic J. Alpha-Particle Therapy for Acute Myeloid Leukemia. *JMIRS.* 2019 Mar 1;50(1):S18.
  80. Rosenblat TL, McDevitt MR, Mulford DA, Pandit-Taskar N, Divgi CR, Panageas KS, et al. Sequential cytarabine and  $\alpha$ -particle immunotherapy with bismuth- $^{213}\text{Bi}$ -lintuzumab (HuM195) for acute myeloid leukemia. *Clin Cancer Res.* 2010 Nov 1;16(21):5303–11.
  81. Jurcic JG, Larson SM, Sgouros G, McDevitt MR, Finn RD, Divgi CR, et al. Targeted  $\alpha$  particle immunotherapy for myeloid leukemia. *Blood.* 2002 Aug 15;100(4):1233–9.
  82. Bethge WA, Wilbur DS, Storb R, Hamlin DK, Santos EB, Brechbiel MW, et al. Radioimmunotherapy with bismuth- $^{213}\text{Bi}$  as conditioning for nonmyeloablative allogeneic hematopoietic cell transplantation in dogs: a dose deescalation study.

- Transplantation. 2004 Aug 15;78(3):352–9.
83. Kneifel S, Cordier D, Good S, Ionescu MCS, Ghaffari A, Hofer S, et al. Local targeting of malignant gliomas by the diffusible peptidic vector 1,4,7,10-tetraazacyclododecane-1-glutaric acid-4,7,10-triacetic acid-substance P. *Clin Cancer Res*. 2006 Jun 15;12(12):3843–50.
  84. Królicki L, Bruchertseifer F, Kunikowska J, Koziara H, Królicki B, Jakuciński M, et al. Safety and efficacy of targeted alpha therapy with <sup>213</sup>Bi-DOTA-substance P in recurrent glioblastoma. *EUR J NUCL MED MOL I*. 2019 Mar 1;46(3):614–22.
  85. Cordier D, Forrer F, Bruchertseifer F, Morgenstern A, Apostolidis C, Good S, et al. Targeted alpha-radionuclide therapy of functionally critically located gliomas with <sup>213</sup>Bi-DOTA-[Thi8, Met(O2)11]- substance P: A pilot trial. *Eur J Nucl Med Mol I*. 2010 Jul 16;37(7):1335–44.
  86. Kratochwil C, Schmidt K, Afshar-Oromieh A, Bruchertseifer F, Rathke H, Morgenstern A, et al. Targeted alpha therapy of mCRPC: Dosimetry estimate of <sup>213</sup>Bismuth-PSMA-617. *Eur J Nucl Med Mol Imaging*. 2018 Jan 1;45(1):31–7.
  87. Hong H, Sun J, Cai W. Radionuclide-Based Cancer Imaging Targeting the Carcinoembryonic Antigen. *Biomark Insights*. 2008 Sep 23;3(10):435–451.
  88. Sathekge M, Knoesen O, Meckel M, Modiselle M, Vorster M, Marx S. <sup>213</sup>Bi-PSMA-617 targeted alpha-radionuclide therapy in metastatic castration-resistant prostate cancer. *Eur J Nucl Med*. 2017 Jun 1;44(6):1099–100.
  89. Verhoeven M, Seimbille Y, Dalm SU. Therapeutic applications of pretargeting. *Pharmaceutics*. 2019 Sep 1;11(9):434.
  90. Parray HA, Shukla S, Samal S, Shrivastava T, Ahmed S, Sharma C, et al. Hybridoma technology a versatile method for isolation of monoclonal antibodies, its applicability across species, limitations, advancement and future perspectives. *Int Immunopharmacol*. 2020 Aug 1;85:106639.
  91. Listek M, Hönow A, Gossen M, Hanack K. A novel selection strategy for antibody producing hybridoma cells based on a new transgenic fusion cell line. *Nat Sci Rep*. 2020 Dec 1;10(1):1–12.
  92. Fichou N, Gouard S, Maurel C, Barbet J, Ferrer L, Morgenstern A, et al. Single-dose anti-CD138 radioimmunotherapy: Bismuth-213 is more efficient than lutetium-177 for treatment of multiple myeloma in a preclinical model. *Front Med*. 2015;2(76).
  93. Fazel J, Rötzer S, Seidl C, Feurecker B, Autenrieth M, Weirich G, et al. Fractionated intravesical radioimmunotherapy with <sup>213</sup>Bi-anti-EGFR-MAB is effective without toxic side-effects in a nude mouse model of advanced human bladder carcinoma. *Cancer Biol Ther*. 2015 Oct 1;16(10):1526–34.
  94. Holliger P, Hudson PJ. Engineered antibody fragments and the rise of single domains. *Nat Biotechnol*. 2005 Sep;23(9):1126–36.
  95. Adams GP, Shaller CC, Chappell LL, Wu C, Horak EM, Simmons HH, et al. Delivery of the  $\alpha$ -emitting radioisotope bismuth-213 to solid tumors via single-chain Fv and diabody molecules. *Nucl Med Biol*. 2000;27(4):339–46.
  96. J. Strosberg, G. El-Haddad, E. Wolin, A. Hendifar, J. Yao, B. Chasen EM, P.L. Kunz, M.H. Kulke, H. Jacene, D. Bushnell, T.M. O'Dorisio RPB, H.R. Kulkarni, M. Caplin, R. Lebtahi, T. Hobday, E. Delpassand EVC, A. Benson, R. Srirajaskanthan, M. Pavel, J. Mora, J. Berlin, E. Grande NR, E. Seregni, K. Öberg, M. Lopera Sierra, P. Santoro, T. Thevenet JLE, P. Ruzsniowski, D. Kwekkeboom, and E. Krenning for the N-1 TI. Phase 3 Trial of <sup>177</sup>Lu-Dotatate for Midgut Neuroendocrine Tumors. *N ENGL J MED*. 2017;2(376):135–35.
  97. Bidwell GL, Raucher D. Therapeutic peptides for cancer therapy. Part I - Peptide inhibitors of signal transduction cascades. *Expert Opin Drug Deliv*. 2009 Oct;6(10):1033–47.
  98. McGregor DP. Discovering and improving novel peptide therapeutics. *Curr Opin Pharmacol*. 2008 Oct;8(5):616–9.
  99. Jiao R, Allen KJH, Malo ME, Rickles D, Dadachova E. Evaluating the combination of radioimmunotherapy and immunotherapy in a melanoma mouse model. *Int J Mol Sci*. 2020 Feb 1;21(3):773.
  100. Nosanchuk JD, Jeyakumar A, Ray A, Revskaya E, Jiang Z, Bryan RA, et al. Structure-function analysis and therapeutic efficacy of antibodies to fungal melanin for melanoma radioimmunotherapy. *Nat Sci Rep*. 2018 Dec 1;8(1):5466.

101. Gustafsson-Lutz A, Bäck T, Aneheim E, Hultborn R, Palm S, Jacobsson L, et al. Therapeutic efficacy of  $\alpha$ -radioimmunotherapy with different activity levels of the <sup>213</sup>Bi-labeled monoclonal antibody MX35 in an ovarian cancer model. *EJNMMI Res.* 2017;7(1):38.
102. Revskaya E, Jiang Z, Morgenstern A, Bruchertseifer F, Sesay M, Walker S, et al. A Radiolabeled Fully Human Antibody to Human Aspartyl (Asparaginy)  $\beta$ -Hydroxylase Is a Promising Agent for Imaging and Therapy of Metastatic Breast Cancer. *Cancer Biother Radiopharm.* 2017 Mar 1;32(2):57–65.
103. Derrien A, Gouard S, Maurel C, Gaugler MH, Bruchertseifer F, Morgenstern A, et al. Therapeutic efficacy of alpha-RIT using a <sup>213</sup>Bi-anti-hCD138 antibody in a mouse model of ovarian peritoneal carcinomatosis. *Front Med.* 2015;2:88.
104. Feuerrecker B, Michalik M, Hundshammer C, Schwaiger M, Bruchertseifer F, Morgenstern A, et al. Assessment of <sup>213</sup>Bi-anti-EGFR MAb treatment efficacy in malignant cancer cells with [<sup>1-13</sup>C]pyruvate and [<sup>18</sup>F]FDG. *Nat Sci Rep.* 2019 Dec 1;9(8294).
105. Ménager J, Gorin JB, Maurel C, Drujont L, Gouard S, Louvet C, et al. Combining  $\alpha$ -radioimmunotherapy and adoptive T cell therapy to potentiate tumor destruction. *PLoS One.* 2015 Jun 22;10(6):e0130249.
106. Teiluf K, Seidl C, Blechert B, Gaertner FC, Gilbertz KP, Fernandez V, et al.  $\alpha$ -radioimmunotherapy with <sup>213</sup>Bi-anti-CD38 immunoconjugates is effective in a mouse model of human multiple myeloma. *Oncotarget.* 2015;6(7):4692–703.
107. Song H, Hedayati M, Hobbs RF, Shao C, Bruchertseifer F, Morgenstern A, et al. Targeting aberrant DNA double-strand break repair in triple-negative breast cancer with alpha-particle emitter radiolabeled anti-EGFR antibody. *Mol Cancer Ther.* 2013 Oct;12(10):2043–54.
108. Roscher M, Hormann I, Leib O, Marx S, Moreno J, Miltner E, et al. Targeted alpha-therapy using [<sup>213</sup>Bi]anti-CD20 as novel treatment option for radio-and chemoresistant non-Hodgkin lymphoma cells. *Oncotarget.* 2013 Feb 24;4(2):218–30.
109. Pagel JM, Kenoyer AL, Bäck T, Hamlin DK, Wilbur DS, Fisher DR, et al. Anti-CD45 pretargeted radioimmunotherapy using bismuth-213: High rates of complete remission and long-term survival in a mouse myeloid leukemia xenograft model. *Blood.* 2011 Jul 21;118(3):703–11.
110. Allen BJ, Abbas Rizvi SM, Qu CF, Smith RC. Targeted alpha therapy approach to the management of pancreatic cancer. *Cancers (Basel).* 2011 Jun;3(2):1821–43.
111. Park SI, Shenoi J, Page JM, Hamlin DK, Wilbur DS, Orgun N, et al. Conventional and pretargeted radioimmunotherapy using bismuth-213 to target and treat non-Hodgkin lymphomas expressing CD20: A preclinical model toward optimal consolidation therapy to eradicate minimal residual disease. *Blood.* 2010 Nov 18;116(20):4231–9.
112. Lingappa M, Song H, Thompson S, Bruchertseifer F, Morgenstern A, Sgouros G. Immunoliposomal delivery of <sup>213</sup>Bi for  $\alpha$ -emitter targeting of metastatic breast cancer. *Cancer Res.* 2010 Sep 1;70(17):6815–23.
113. Drecol E, Gaertner FC, Miederer M, Blechert B, Vallon M, Müller JM, et al. Treatment of peritoneal carcinomatosis by targeted delivery of the radio-labeled tumor homing peptide <sup>213</sup>Bi-DTPA-[F3]2 into the nucleus of tumor cells. *PLoS One.* 2009 May 27;4(5):e5715.
114. Li Y, Rizvi SMA, Ranson M, Allen BJ. <sup>213</sup>Bi-PAI2 conjugate selectively induces apoptosis in PC3 metastatic prostate cancer cell line and shows anti-cancer activity in a xenograft animal model. *Br J Cancer.* 2002 Apr 8;86(7):1197–203.
115. Fjelde A, Id M, Saidi A, Torgue J, Heyerdahl H, Stallons TAR, et al. Targeted alpha therapy for chronic lymphocytic leukaemia and non-Hodgkin's lymphoma with the anti-CD37 radioimmunoconjugate <sup>212</sup>Pb-NNV003. *PLoS One.* 15(3):e023.
116. Ebbers SC, Braat AJAT, Moelker A, Stokkel MPM, Lam MGEH, Barentsz MW. Intra-arterial versus standard intravenous administration of lutetium-177-DOTA-octreotate in patients with NET liver metastases: Study protocol for a multicenter, randomized controlled trial (LUTIA trial). *Trials.* 2020 Feb 5;21(1).
117. Graf J, Pape UF, Jann H, Denecke T, Arsenic R, Brenner W, et al. Prognostic Significance of Somatostatin Receptor Heterogeneity in Progressive Neuroendocrine Tumor Treated with Lu-177 DOTATOC or Lu-177 DOTATATE. *Eur J Nucl Med Mol I.* 2020 Apr 1;47(4):881–94.
118. Delpassand ES, Samarghandi A, Zamanian S, Wolin EM, Hamiditabar M, Espenan GD, et al. Peptide receptor radionuclide

- therapy with <sup>177</sup>Lu-DOTATATE for patients with somatostatin receptor-expressing neuroendocrine tumors: The first US phase 2 experience. *Pancreas*. 2014;43(4):518–25.
119. Allen BJ, Raja C, Rizvi S, Li Y, Tsui W, Graham P, et al. Intralesional targeted alpha therapy for metastatic melanoma. *Cancer Biol Ther*. 2005 Dec;4(12):1318–24.
  120. Finn LE, Levy M, Orozco JJ, Park JH, Atallah E, Craig M, et al. A Phase 2 Study of Actinium-225 (<sup>225</sup>Ac)-Lintuzumab in Older Patients with Previously Untreated Acute Myeloid Leukemia (AML) Unfit for Intensive Chemotherapy. *Blood*. 2017 Dec 7;130(Supplement 1):2638.
  121. Jurcic JG, Ravandi F, Pagel JM, Park JH, Smith BD, Douer D, et al. Phase I trial of  $\alpha$ -particle therapy with actinium-225 (<sup>225</sup>Ac)-lintuzumab (anti-CD33) and low-dose cytarabine (LDAC) in older patients with untreated acute myeloid leukemia (AML). *J Clin Oncol*. 2015 May 20;33(15\_suppl):7050–7050.
  122. Juzeniene A, Stenberg VY, Bruland ØS, Larsen RH. Preclinical and Clinical Status of PSMA-Targeted Alpha Therapy for Metastatic Castration-Resistant Prostate Cancer. *Cancers (Basel)*. 2021 Feb 13;13(4):779.
  123. Allen BJ, Raja C, Rizvi S, Li Y, Tsui W, Graham P, et al. Intralesional targeted alpha therapy for metastatic melanoma. *Cancer Biol Ther*. 2005;4(12):1318–24.
  124. Allen BJ, Singla AA, Rizvi SMA, Graham P, Bruchertseifer F, Apostolidis C, et al. Analysis of patient survival in a Phase I trial of systemic targeted  $\alpha$ -therapy for metastatic melanoma. *Immunotherapy*. 2011 Sep 13;3(9):1041–50.
  125. Raja C, Graham P, Abbas Rizvi SM, Song E, Goldsmith H, Thompson J, et al. Interim analysis of toxicity and response in phase 1 trial of systemic targeted alpha therapy for metastatic melanoma. *Cancer Biol Ther*. 2007;6(6):846–52.
  126. Jansen K, Heirbaut L, Cheng JD, Joossens J, Ryabtsova O, Cos P, et al. Selective inhibitors of fibroblast activation protein (FAP) with a (4-quinolinoyl)-glycyl-2-cyanopyrrolidine scaffold. *ACS Med Chem Lett*. 2013 May 9;4(5):491–6.
  127. Giesel FL, Kratochwil C, Lindner T, Marschalek MM, Loktev A, Lehnert W, et al. <sup>68</sup>Ga-FAPI PET/CT: Biodistribution and preliminary dosimetry estimate of 2 DOTA-containing FAP-targeting agents in patients with various cancers. *J Nucl Med*. 2019;60(3):386–92.
  128. Lindner T, Loktev A, Altmann A, Giesel F, Kratochwil C, Debus J, et al. Development of quinoline-based theranostic ligands for the targeting of fibroblast activation protein. *J Nucl Med*. 2018 Sep 1;59(9):1415–22.
  129. Loktev A, Lindner T, Mier W, Debus J, Altmann A, Jäger D, et al. A tumor-imaging method targeting cancer-associated fibroblasts. *J Nucl Med*. 2018 Sep 1;59(9):1423–9.
  130. Jaggi JS, Seshan S V., McDevitt MR, Sgouros G, Hyjek E, Scheinberg DA. Mitigation of radiation nephropathy after internal  $\alpha$ -particle irradiation of kidneys. *Int J Radiat Oncol Biol Phys*. 2006 Apr 1;64(5):1503–12.
  131. Chatal JF, Davodeau F, Cherel M, Barbet J. Different ways to improve the clinical effectiveness of radioimmunotherapy in solid tumors. *J Cancer Res Ther*. 2009 Sep;5 Suppl 1:S36–40.
  132. Song EY, Abbas Rizvi SM, Qu CF, Raja C, Brechbiel MW, Morgenstern A, et al. Pharmacokinetics and toxicity of <sup>213</sup>Bi-labeled PAI2 in preclinical targeted alpha therapy for cancer. *Cancer Biol Ther*. 2007 Jun;6(6):898–904.
  133. Bendre S, Zhang Z, Kuo H-T, Rousseau J, Zhang C, Merckens H, et al. Evaluation of Met-Val-Lys as a Renal Brush Border Enzyme-Cleavable Linker to Reduce Kidney Uptake of <sup>68</sup>Ga-Labeled DOTA-Conjugated Peptides and Peptidomimetics. *Molecules*. 2020 Aug 25;25(17):3854.
  134. Suzuki C, Uehara T, Kanazawa N, Wada S, Suzuki H, Arano Y. Preferential Cleavage of a Tripeptide Linkage by Enzymes on Renal Brush Border Membrane To Reduce Renal Radioactivity Levels of Radiolabeled Antibody Fragments. *J Med Chem*. 2018 Jun 28;61(12):5257–68.